Journal of Medicinal Chemistry

Article

Cite This: J. Med. Chem. XXXX, XXX, XXX−XXX

pubs.acs.org/jmc

[^{3}H]UR-DEBa176: A 2,4-Diaminopyrimidine-Type Radioligand Enabling Binding Studies at the Human, Mouse, and Rat Histamine H_4 Receptors

Edith Bartole,*[,†] Timo Littmann,[†,§] Miho Tanaka,[‡] Takeaki Ozawa,[‡] Armin Buschauer,[†,∥] and Günther Bernhardt*[,†]

[†]Institute of Pharmacy, University of Regensburg, D-93053 Regensburg, Germany

[‡]Department of Chemistry, School of Science, University of Tokyo, 7-3-1 Bunkyo-ku, Hongo, Tokyo 113-0033, Japan

Supporting Information

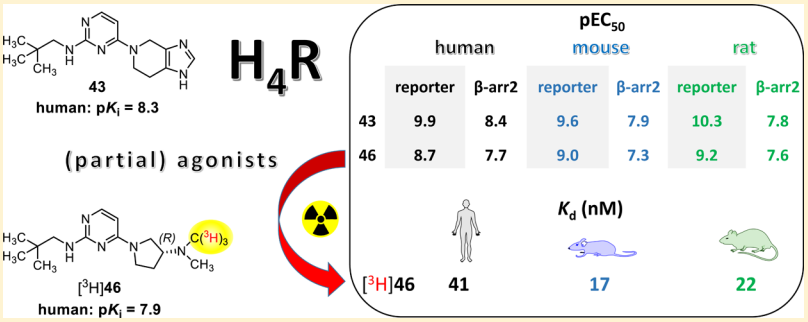

ABSTRACT: Differences in sequence homology between human (h), mouse (m), and rat (r) histamine H_4 receptors (H_4R) cause discrepancies regarding affinities, potencies, and/or efficacies of ligands and therefore compromise translational animal models and the applicability of radioligands. Aiming at a radioligand enabling robust and comparative binding studies at the h/m/rH_4Rs, 2,4-diaminopyrimidines were synthesized and pharmacologically investigated. The most notable compounds identified were two (partial) agonists with comparable potencies at the h/m/rH_4Rs: UR-DEBa148 (*N*-neopentyl-4-(1,4,6,7-tetrahydro-5*H*-imidazo[4,5-*c*]pyridin-5-yl)pyrimidin-2-amine bis(2,2,2-trifluoroacetate), **43**), the most potent [pEC_{50} (reporter gene assay) = 9.9/9.6/10.3] compound in the series being slightly G-protein biased and UR-DEBa176 [(*R*)-4-[3-(dimethylamino)pyrrolidin-1-yl]-*N*-neopentylpyrimidin-2-amine bis(2,2,2-trifluoroacetate), **46**, pEC_{50} (reporter gene assay) = 8.7/9.0/9.2], a potential "cold" form of a tritiated H_4R ligand. After radiolabeling, binding studies with [^{3}H]UR-DEBa176 ([^{3}H]**46**) at the h/m/rH_4Rs revealed comparable K_d values (41/17/22 nM), low nonspecific binding (11−17%, ~K_d), and fast associations/dissociations (25−30 min) and disclosed [^{3}H]UR-DEBa176 as useful molecular tool to determine h/m/rH_4R binding affinities for H_4R ligands.

INTRODUCTION

The human histamine H_4 receptor (hH_4R) was discovered at the turn of the millennium as the latest member of the histamine receptor family (H_{1-4}Rs)[1−7] and is expected to be a promising target for the treatment of disorders of the immune system (e.g., rheumatoid arthritis, bronchial asthma).[8,9] The expression and a potential physiological role of the H_4R in the brain was controversially discussed in the literature.[10] For investigations on the (patho)physiology of the H_4R, mouse and rat became the most important laboratory animals.[11] However, the pharmacological evaluation of the rodent histamine H_4 receptors (mH_4R, rH_4R) is compromised by species-dependent discrepancies regarding the potencies (e.g., **1**, **2**,[12] and **3**[13]) and/or the quality of action (e.g., **4**,[14] **5**,[15] and **6**[14]) of standard ligands for the hH_4R (Figure 1).[16−18] These differences are probably caused by the substantially different constitutive activities of the H_4R species orthologs[4,17,19,20] and the low sequence homology (68−69%[21]) of the mH_4R and the rH_4R with the hH_4R. For radioligand binding studies on the H_4R, only four radioligands [[^{3}H]**1**,[4,5,16,21,22] [^{3}H]**2**,[12] [^{3}H]**5**,[14,23] and [^{125}I]iodophenpropit[14] (not shown)] were reported, but their use is limited: because of the low potencies at the rodent receptors (Figure 1) in combination with the specific activity of 10−25 Ci/mmol of the commercially available labeled histamine [^{3}H]**1**, relatively high amounts of radioligand and the receptor protein are required for binding studies.[12] Additionally, binding experiments with [^{3}H]**1** revealed either significantly different binding constants [K_d (nM): 5−9 (hH_4R); 42−78 (mH_4R); 134−178 (rH_4R)][21−24] at the receptor orthologs or failed[16] at the mouse and rat H_4Rs. Iodophenpropit is a high-affinity hH_4R ligand (pK_i: 7.9[14]). Nonetheless, the use of [^{125}I]iodophenpropit as a radioligand is limited because of the poor chemical stability, short half-life of

Received: August 14, 2019

DOI: 10.1021/acs.jmedchem.9b01342
J. Med. Chem. XXXX, XXX, XXX−XXX

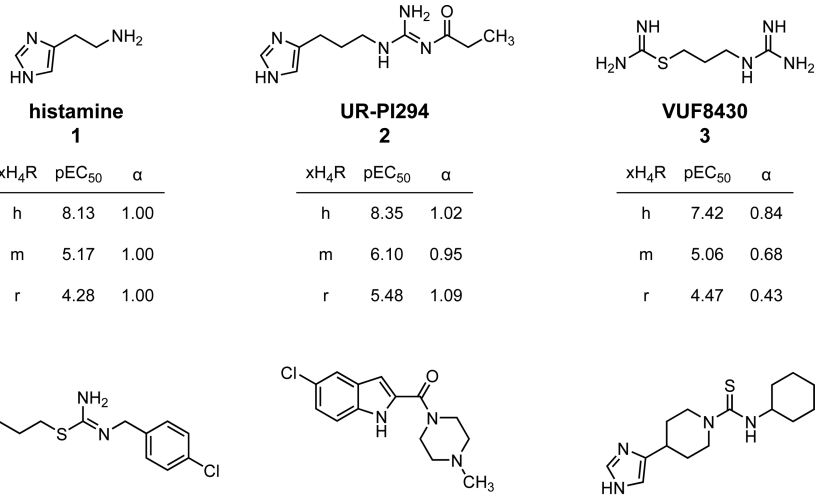

histamine
1

xH_4R	pEC_{50}	α
h	8.13	1.00
m	5.17	1.00
r	4.28	1.00

UR-PI294
2

xH_4R	pEC_{50}	α
h	8.35	1.02
m	6.10	0.95
r	5.48	1.09

VUF8430
3

xH_4R	pEC_{50}	α
h	7.42	0.84
m	5.06	0.68
r	4.47	0.43

clobenprobit
4

xH_4R	$pEC_{50}/(pK_b)$	α
h	7.65	0.45
m	6.07	0.20
r	(6.28)	0

JNJ7777120
5

xH_4R	$pEC_{50}/(pK_b)$	α
h	(7.60)	-0.39
m	6.10	0.44
r	6.13	0.24

thioperamide
6

xH_4R	pK_b	α
h	6.83	-1.39
m	7.12	0
r	6.44	0

Figure 1. Structures and functional data of known hH_4R ligands obtained from [^{35}S]-GTPγS-binding assays[17] on the human (h), mouse (m), and rat (r) H_4R receptors.

the ^{125}I-label (59.4 days) in comparison to ^{3}H-labeled ligands (12.4 years), and the need to follow special safety precautions (e.g., shielding) during preparation and handling.[12] The radiolabeled agonist [^{3}H]**2**[12] (Figure 1) was developed for the hH_3R and hH_4R with comparably high affinities at both receptor subtypes. By contrast, the potency of **2** at the mH_4R and rH_4R was in the three- to four-digit nM range (Figure 1) in a functional assay with a proximal readout ([^{35}S]-GTPγS assay[17]). Therefore, [^{3}H]**2** is inappropriate for radioligand binding experiments at the mH_4R or rH_4R. Binding studies with [^{3}H]**5** revealed comparably high affinities at the h/m/rH_4Rs.[23] By contrast, saturation binding experiments with [^{3}H]**5** in our laboratory[25] were only feasible at the hH_4R expressed in *Sf*9 membranes, accompanied by a high level of nonspecific binding (30−40% of total binding around the K_d).[25] Additionally, the substantial species-dependent differences in the quality of action of **5** in several functional assays (e.g., [^{35}S]-GTPγS[17] and luciferase reporter gene[26] assays) may compromise H_4R radioligand binding studies across species. Moreover, [^{3}H]**5** is not commercially available, and a customer commissioned synthesis would be expensive.[25] Because of the aforementioned drawbacks of the reported radioligands for the H_4R, we were aiming at a new radioligand as a molecular tool, allowing comparative and robust binding studies at the h/m/rH_4Rs with the following characteristics: convenient synthesis (e.g., by methylation[27] or propionylation[28] in the last synthetic step), high degree of chemical/radiochemical purity and stability, high specific activity, low nonspecific binding (<20% of total binding), binding constants (K_d values) in the one- to two-digit-nM range, and comparable intrinsic activities at the h/m/rH_4Rs. Therefore, a set of 2,4-diaminopyrimidines was prepared, based on the structure of **33**[29,30] (Scheme 1), which was reported as an equipotent agonist at the human and rodent H_4Rs.[30] For structural modification, (cyclic) aliphatic amines, histamine **1**, and some of its homologs were introduced in position 4 of the 2,4-diaminopyrimidine scaffold, whereas in position 2, a neopentylamine moiety was kept constant (Scheme 1). Some cyclic aliphatic amines were methylated, propionylated, or guanidinylated (Scheme 1). Initially, the structure−affinity relationships of the small library were explored at the hH_4R. The selection of target structures for radiolabeling was based on the results of various functional assays at the human and the rodent H_4R species variants.

RESULTS AND DISCUSSION

Chemistry. Heating the amine precursors **7**−**18** [structures (Schemes S1−S3 and Figure S1), source or synthesis see the Supporting Information] with the 2,4-dichloropyrimidine **19** (Scheme 1) in a microwave reactor or in a round-bottom flask[29] under basic conditions in *i*-PrOH, the intermediates **20**−**31** (Scheme 1) were prepared (synthesis see the Supporting Information). Subsequently, a second nucleophilic substitution reaction of **20** with an excess of 2,2-dimethylpropan-1-amine was performed in a protic solvent (*i*-PrOH) and in the presence of *N*,*N*-diisopropylethylamine (DIPEA) using a microwave reactor over 6 hours to get the Boc-protected 2,4-diaminopyrimidine **32** (Scheme 1). After removal of the protection group under acidic conditions [trifluoroacetic acid (TFA)], the desired 2,4-diaminopyrimidine **33** was obtained in good yield (78.4%). Basically, target compounds **34**−**44** were prepared under comparable conditions, starting with intermediates **21**−**31**. For the preparation of **44**, deprotection was unnecessary. Treating the Boc-protected intermediate **32** with an excess of $LiAlH_4$ (5 equiv) in anhydrous tetrahydrofuran (THF),[31] the monomethylated 2,4-diaminopyrimidine **45** was obtained in moderate yield (43%) after refluxing for 7 h (Scheme 1). Target compounds **33**−**35** were methylated under Eschweiler−Clarke conditions using formaldehyde and formic acid to give the mono- or dimethylated 2,4-

DOI: 10.1021/acs.jmedchem.9b01342
J. Med. Chem. XXXX, XXX, XXX−XXX

Scheme 1. Synthesis of the 2,4-Diaminopyrimidines 33−52[a]

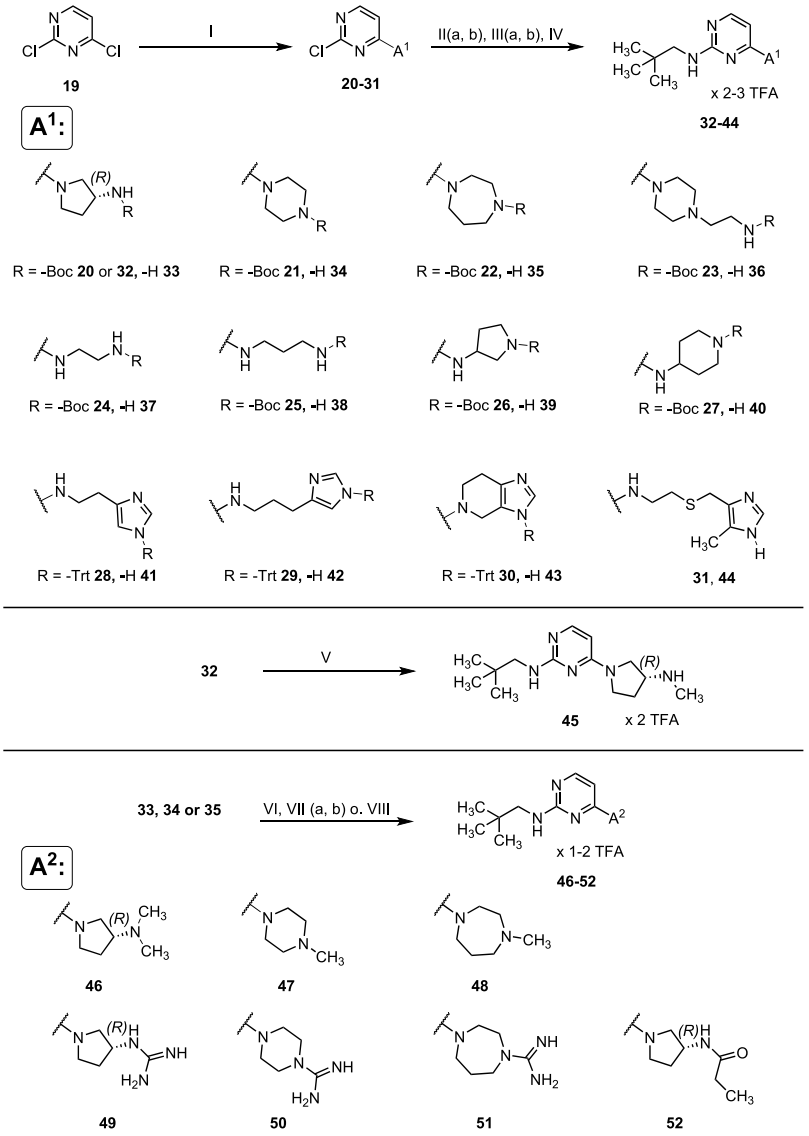

[a]Reagents and conditions: (I) **7**−**18** (see the Supporting Information), DIPEA, *i*-PrOH, 120 °C (microwave), 1 h, 73% (**20**), or 55−85 °C, 4−20 h, 64−95% (**21**−**31**) (see the Supporting Information); (IIa) **20**, 2,2-dimethylpropan-1-amine, DIPEA, *i*-PrOH, 130 °C (microwave), 6 h, 96.2% (**32**), (IIb) **32**, TFA, DCM, rt, 8 h, 78.4% (**33**); (IIIa) **21**−**30**, 2,2-dimethylpropan-1-amine, DIPEA, *i*-PrOH, 120−140 °C (microwave), 4−11 h, (IIIb) TFA, DCM, rt, 7−18 h, 14−65% (**34**−**43**); (IV) **31**, 2,2-dimethylpropan-1-amine, DIPEA, *i*-PrOH, 120 °C (microwave), 4 h, 17.4% (**44**); (V) $LiAlH_4$, anhydrous THF, 70 °C, 7 h, 43% (**45**). (VI) **33**−**35**, formic acid/formamide 1/1 (v/v), 95 °C, 3−5 h, 49−73% (**46**−**48**); (VIIa) **33**−**35**, 1,3-bis(*tert*-butoxycarbonyl)-2-methyl-2-thiopseudourea, $HgCl_2$, TEA, DCM, rt, 6 h, (VIIb) TFA, DCM, rt, 5−7 h, 26−40% (**49**−**51**); (VIII) **33**, 1-propionylpyrrolidine-2,5-dione, DIPEA, DCM, rt, 24 h, 57% (**52**).

diaminopyrimidines **46**−**48** (Scheme 1). The guanidinylations of **33**−**35** using 1,3-bis(*tert*-butoxycarbonyl)-2-methyl-2-thiopseudourea[25] and $HgCl_2$ under basic conditions were performed as previously described.[32] Subsequent deprotection under acidic conditions led to **49**−**51** (Scheme 1). Compound **33** was propionylated under basic conditions using 1-propionylpyrrolidine-2,5-dione, according to a previously described procedure[28] to give **52** (Scheme 1). All target compounds (Scheme 1) were purified by preparative high-performance liquid chromatography (HPLC) to obtain the respective TFA salts in high chemical purity (>96%) (for details see the Experimental Section).

Investigations on the Chemical Stability of 43, 46, 48, and 49. The chemical stability of **43** (UR-DEBa148), **46** (UR-DEBa176), **48**, and **49** was investigated in PBS (pH 7.4) at 23 °C over a time period of 24 h. Under these conditions, the investigated 2,4-diaminopyrimidines proved stable (graphs see Figures S33−S36 in the Supporting Information, for details see chemical stability in the Experimental Section).

Affinities at the Human H_4R and Subtype Selectivity over the Human $H_{1-3}Rs$. With the 2,4-diaminopyrimdines, radioligand competition binding experiments were performed to investigate their structure−affinity relationships at the hH_4R and their subtype selectivity over the $hH_{1-3}Rs$. The binding constants (pK_i values) at the $hH_{1-4}R$, expressed in membrane preparations of *Sf*9 insect cells, are presented in Table 1. The structures of the synthesized 2,4-diaminopyrimidines are depicted in Scheme 1. The (*R*)-3-aminopyrrolidine **33**[29,30] and homopiperazine **35**[29] revealed comparable high affinities at the hH_4R (pK_i = 8.07 and 7.88, respectively). Selectivity

DOI: 10.1021/acs.jmedchem.9b01342
J. Med. Chem. XXXX, XXX, XXX−XXX

Table 1. Affinity and Subtype Selectivity of the 2,4-Diaminopyrimidines at the Human H_{1-4}Rs

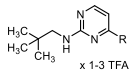

No.	R	pK_i				Selectivity ratios of K_i($H_{2\text{-}4}$Rs)
		hH$_4$R	hH$_3$R	hH$_2$R	hH$_1$R	H$_4$R / H$_3$R / H$_2$R
33		8.07 ± 0.10[a]	7.86 ± 0.14[c]	< 5.0	< 5.0	1 / 1.7 / > 1000
34		6.73 ± 0.03 [a]	< 5.0[c]	< 5.0	< 5.0	1 / > 53 / > 53
35		7.88 ± 0.06[b]	6.27 ± 0.03[d]	< 5.0	< 5.0	1 / 48 / > 750
36	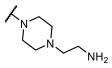	< 5.0[a]	< 5.0[c]	< 5.0	< 5.0	- / - / -
37		6.69 ± 0.14[a]	6.16 ± 0.04[c]	< 5.0	< 6.0	1 / 3 / > 40
38	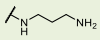	7.44 ± 0.05[b]	5.25 ± 0.02[c,d]	< 6.0	< 5.0	1 / 118 / > 27
39		6.51 ± 0.02[b]	6.69 ± 0.2[c,d]	< 6.0	< 5.0	1.2 / 1 / > 4
40		5.72 ± 0.16[b]	5.46 ± 0.01[c,d]	< 5.0	< 5.0	1 / 1.6 / > 4.7
41		6.69 ± 0.07[b]	8.02 ± 0.07[d]	n.d.	n.d.	22 / 1 / -
42	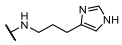	6.35 ± 0.04[b]	8.03 ± 0.04[d]	n.d.	n.d.	48 / 1 / -
43		8.29 ± 0.13[a]	8.48 ± 0.04[c]	< 5.0	< 5.0	1.7 / 1 / > 1800
44	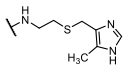	< 5.0[a]	< 5.0[c]	6.25 ± 0.03	< 6.0	> 17 / > 17 / 1
45		8.42 ± 0.07[b]	7.56 ± 0.11[c,d]	< 5.0	< 5.0	1 / 7.4 / > 2500
46		7.93 ± 0.04[a]	6.84 ± 0.07[c]	< 6.0	< 5.0	1 / 13 / > 84
47		6.94 ± 0.08[a]	5.26 ± 0.04[c]	< 5.0	< 5.0	1 / 47 / > 85
48		7.20 ± 0.05[a]	5.62 ± 0.14[c]	< 6.0	< 5.0	1/ 30 / > 16
49	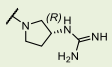	7.16 ± 0.06[a,b]	5.95 ± 0.07[c]	< 6.0	< 5.0	1 / 16 / > 14
50		6.21 ± 0.01[a]	5.22 ± 0.04[c]	< 5.0	< 6.0	1 / 10 / > 16
51		5.57 ± 0.13[a]	< 5.0[c]	< 5.0	< 5.0	1 / > 3.4 / > 3.4
52	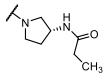	5.58 ± 0.17[b]	5.52 ± 0.15[c,d]	< 5.0	< 5.0	1 / 1.2 / > 3.6

Competition binding determined at cell membranes of *Sf9* insect cells expressing the hH$_4$R + Gi$_{\alpha 2}$ + $\beta_1\gamma_2$, hH$_3$R + Gi$_{\alpha 2}$ + $\beta_1\gamma_2$, hH$_2$R-Gs$_{\alpha s}$ or hH$_1$R + RGS4. Radioligands for hH$_4$R: [^{3}H]**1** (10[a] or 40 nM[b]); hH$_3$R: [^{3}H]*N*α-methylhistamine (3 nM)[c] or [^{3}H]**2**[12] (2 nM)[d]; hH$_2$R: [^{3}H]UR-DE257[28] (20 nM); hH$_1$R: [^{3}H]pyrilamine (5 nM). The pK_i values represent means ± SEM. Data represent 2 (for pK_i values ≤ 6.25) or 3−4 (for pK_i values > 6.25) independent experiments, each performed in triplicates. n.d. means not determined.

DOI: 10.1021/acs.jmedchem.9b01342
J. Med. Chem. XXXX, XXX, XXX−XXX

Table 2. Potencies and Efficacies of the 2,4-Diaminopyrimidines at the Human, Mouse, and Rat H_4R in Luciferase Reporter Gene- and β-Arrestin2 Recruitment Assays[a]

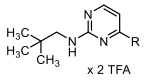

No.	R	pEC_{50} / (α)					
		hH_4R		mH_4R		rH_4R	
		reporter gene	β-arr2	reporter gene	β-arr2	reporter gene	β-arr2
1	-	7.77 ± 0.12[26]	7.47 ± 0.12	7.06 ± 0.13[26]	5.63± 0.07	6.53 ± 0.04[26]	5.43 ± 0.06
		(1.00)	(1.00)	(1.00)	(1.00)	(1.00)	(1.00)
33		8.45 ± 0.14	7.84 ± 0.03	8.38 ± 0.07	6.87 ± 0.11	8.75 ± 0.12	7.47 ± 0.11
		(0.85 ± 0.04)	(0.38 ± 0.03)	(0.99 ± 0.09)	(0.83 ± 0.03)	(0.98 ± 0.01)	(0.31 ± 0.04)
35		7.74 ± 0.09	7.37 ± 0.09	7.29 ± 0.06	6.45 ± 0.04	7.03 ± 0.08	6.19 ± 0.11
		(0.91 ± 0.05)	(0.43 ± 0.02)	(0.96 ± 0.05)	(0.68 ± 0.01)	(1.01 ± 0.01)	(0.36 ± 0.01)
38	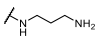	7.53 ± 0.10	7.40 ± 0.14	7.29 ± 0.10	5.97 ± 0.06	7.64 ± 0.07	6.72 ± 0.03
		(0.94 ± 0.06)	(0.67 ± 0.02)	(1.06 ± 0.07)	(0.65 ± 0.02)	(0.94 ± 0.07)	(0.71 ± 0.01)
43		9.91 ± 0.11	8.38 ± 0.09	9.60 ± 0.06	7.94 ± 0.01	10.30 ± 0.10	7.78 ± 0.05
		(0.58 ± 0.02)	(0.19 ± 0.02)	(0.77 ± 0.06)	(0.58 ± 0.04)	(0.98 ± 0.02)	(0.36 ± 0.01)
45		9.22 ± 0.01	8.16 ± 0.09	8.96 ± 0.05	7.59 ± 0.03	9.21 ± 0.05	7.53 ± 0.10
		(0.54 ± 0.06)	(0.12 ± 0.02)	(0.96 ± 0.01)	(0.58 ± 0.03)	(0.84 ± 0.08)	(0.11 ± 0.01)
46		8.72 ± 0.09	7.73 ± 0.12	8.99 ± 0.05	7.29 ± 0.06	9.19 ± 0.10	7.59 ± 0.07
		(0.64 ± 0.01)	(0.25 ± 0.01)	(0.93 ± 0.03)	(0.74 ± 0.05)	(1.05 ± 0.02)	(0.68 ± 0.05)
48		7.71 ± 0.07	6.86 ± 0.01	7.45 ± 0.05	6.08 ± 0.01	8.93 ± 0.10	6.48 ± 0.11
		(0.87 ±0.02)	(0.34 ± 0.03)	(0.90 ± 0.04)	(0.72 ± 0.05)	(0.98 ± 0.01)	(0.75 ± 0.03)
49	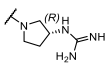	7.45 ± 0.04	7.05 ± 0.09	8.21 ± 0.19	6.64 ± 0.13	8.86 ± 0.13	6.84 ± 0.14
		(0.91 ± 0.04)	(0.44 ± 0.02)	(0.92 ± 0.03)	(0.72 ± 0.05)	(0.99 ± 0.02)	(0.92 ± 0.07)

[a]Data of luciferase reporter gene assay, using HEK293-SF-hH_4R-His6-CRE-Luc, HEK293T-SF-mH_4R-His6-CRE-Luc, or HEK293T-SF-rH_4R-His6-CRE-Luc cells and β-arrestin2 recruitment assay, using HEK293T-β-arr2-xH_4R cells (x = h, m, r). The intrinsic activity (α) of histamine **1** was set to 1.0 and α values of other compounds were referred to this value. Data (mean values ± SEM) were determined in 3−6 independent experiments, each performed in duplicates or triplicates.

over the hH_3R was improved for **35** (≈28-fold compared to **33**), whereas **33** was almost equi-affinic. In comparison to **35**, the hH_4R affinity of the piperazine **34**[29] was reduced (≈14-fold), which is remarkable because the difference is only one methylene group in the aliphatic ring. The selectivity over hH_3R was comparable. By introducing an ethylenediamine moiety into **34**, and thereby adding an additional basic primary amine to the eastern part of the molecule and increasing flexibility, the decrease in hH_4R affinity was striking (**36**: pK_i < 5). The coupling of ethylenediamine, 3-aminopyrrolidine, or 4-aminopiperidine to the 4-position of the pyrimidine core (**37**, **39**, and **40**) via the primary amine function was not successful in gaining affinity for the hH_4R and hH_3R (pK_i < 7.0). An additional H-bond donor and/or an increased flexibility in the aliphatic amine motif seemed not to be tolerated by the hH_4R and hH_3R. By contrast, an elongation of the alkine chain, as for the propylenediamine **38**, improved affinity for the hH_4R (≈6-fold compared to **37**), and the selectivity over the hH_3R (118-fold) was striking. Despite the fact that imidazole-containing compounds lack subtype selectivity,[33] in **41**−**44**, the endogenous ligand histamine **1** and some of its homologs, previously used as precursors in the development of hH_4R ligands,[12,34−37] were merged with the 2,4-diaminopyrimidine chemotype. Interestingly, the histamine derivative **41** and homohistamine derivative **42** showed comparably weak hH_4R affinities (pK_i = 6.69 and 6.35, respectively), while selectivity for the hH_3R increased with the elongation of the alkine chain of the histamine analogue (**41**: 22-fold; **42**: 48-fold). Spinaceamine, the rigid congener of histamine **1**, was merged with the 2-arylbenzimidazole chemotype by Johnson & Johnson in 2010 to gain subtype selectivity for the hH_4R (≈1800-fold[37]). With the introduction of spinaceamine in the 4-position of the 2,4-diaminopyrimidines, high affinity for the hH_4R (**43**, UR-DEBa148: pK_i = 8.29) was obtained. Unfortunately, with respect to subtype selectivity, **43** was almost equi-affinic at the hH_3R. Compound **44** revealed weak affinities ($pK_i \leq 6.25$) for all receptor subtypes with a tendency for the hH_2R. Mono (**45**[29])- and dimethylation (**46**, UR-DEBa176) of the pyrrolidine derivative **33** revealed comparably high affinities at the hH_4R (pK_i = 8.42 and 7.93, respectively). Interestingly, the selectivity over the hH_3R increased with the number of introduced methyl groups (**45**: ≈4-fold compared to **33**; **46**: ≈8-fold compared to **33**). Nonetheless, the introduction of methyl groups did not

DOI: 10.1021/acs.jmedchem.9b01342
J. Med. Chem. XXXX, XXX, XXX−XXX

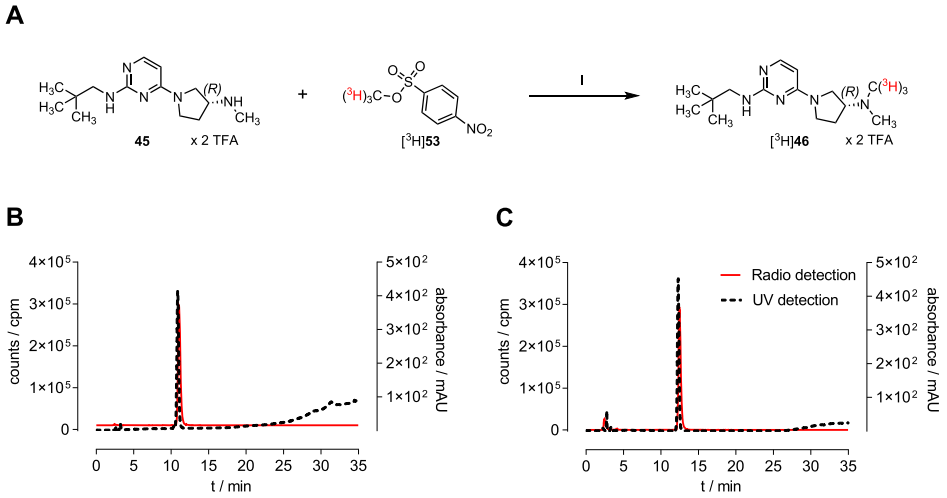

Figure 2. Synthesis (A), analytical characterization (B), and long-term stability (C) of [^{3}H]**46**. (A) Synthesis of [^{3}H]**46** by a monomethylation reaction of the amine precursor **45** with the radiolabeled precursor [^{3}H]**53**. Reagents and conditions (I) K_2CO_3, MeCN, rt, 22 h, 29% (radiochemical yield of [^{3}H]**46**). (B) Chromatograms of [^{3}H]**46**, spiked with the "cold" form **46**, recorded 4 days after synthesis and (C) after 11 months of storage at −20 °C in EtOH/H_2O (70:30) using radiometric and UV detection (for details see Synthesis of radioligand [^{3}H]**46** in the Experimental Section).

increase the bulkiness very much, which might explain this finding. It is more likely that the H-bond donor group in the pyrrolidine derivatives **33** and **45** is more relevant for hH_3R binding than for binding to the hH_4R. Methylation of **34** and **35** did not effect hH_4R affinity (**47**: pK_i = 6.94; **48**: pK_i = 7.20) or subtype selectivity over the hH_3R (**47**: ≈1.1-fold compared to **34**; **48**: ≈1.6-fold compared to **35**). The bioisosteric replacement of amines by a guanidine or an acylguanidine was previously proven effective in case of several selective hH_3R and hH_4R agonists (e.g., **2**,[12] **3**,[13] see Figure 1). This concept was transferred to the 2,4-diaminopyrimidine scaffold. Guanidinylation of **33**, **34**, and **35** led to a decrease in affinity for the hH_4R (**49**: ≈8-fold compared to **33**; **50**: ≈3-fold compared to **34**; **51**: ≈208-fold compared to **35**) and affinities at the hH_3R were weak as well (pK_i < 6.0). This illustrates that the introduction of a bulky but polar H-bond donor group was not well tolerated by the hH_4R and the hH_3R. Strikingly, structural modification by introducing a propionyl moiety into **33**, and thereby reducing the basicity of the molecule, resulted in a marked decrease in affinity for the hH_4R (**52**: ≈306-fold compared to **33**) and the hH_3R (**52**: ≈214-fold compared to **33**). The 2,4-diaminopyrimidines with pK_i values > 6.0 at the hH_4R showed distinct subtype selectivity over the hH_1R and the hH_2R (Table 1). Aiming at a new radioligand for comparative binding studies at hH_4R orthologs, selected 2,4-diaminopyrimidines with pK_i values > 7.0 at the hH_4R (**33**, **35**, **38**, **43**, **45**, **46**, **48**, & **49**) were further assessed in a luciferase reporter gene and β-arrestin2 recruitment assay at the h/m/rH_4Rs. Their ortholog selectivity was studied to identify compounds with comparable potencies and efficacies across the H_4R species variants.

Functional Characterization of Selected 2,4-Diaminopyrimidines at the Human, Mouse, and Rat H_4Rs in the Luciferase Reporter Gene and β-Arrestin2 Recruitment Assays. The potencies (pEC_{50} values) and the efficacies (α values) of the selected 2,4-diaminopyrimidines, which were obtained in the luciferase reporter gene assay and the β-arrestin2 recruitment assay at the H_4R orthologs, are presented in Table 2. Functional assays with distal (reporter gene) and proximal (β-arrestin2) readouts allow a comprehensive investigation on the ortholog selectivity of **33**, **35**, **38**, **43**, **45**, **46**, **48**, and **49**. Of note, because of the distal readout, the luciferase reporter gene assay implies signal amplification.[26] In this study, this was reflected by the discrepancies in the functional profiles of the 2,4-diaminopyrimidines obtained from the different functional assays at all H_4R orthologs. In the luciferase reporter gene assay, all investigated 2,4-diaminopyrimidines (**33**, **35**, **38**, **43**, **45**, **46**, **48**, and **49**) appeared as partial to full agonists with high pEC_{50} values (>7.0) at the h/m/rH_4Rs (Table 2). While **33** and **38** revealed potencies and efficacies comparable between species (balanced functional profiles) in the reporter gene assays, **35**, **48**, and **49** showed unbalanced functional profiles among the H_4R orthologs (Table 2). In the β-arrestin2 recruitment assays, **33**, **35**, **38**, **48**, and **49** appeared as partial agonists at the receptor orthologs, but potencies, especially at the mouse and/or rat H_4Rs were weak (pEC_{50} < 7.0) (Table 2). By contrast, the spinaceamine **43** (UR-DEBa148) showed (partial) agonistic activities in the sub-nM range in the luciferase reporter gene assays and in the one- to two-digit-nM range in the β-arrestin2 recruitment assays at the h/m/rH_4Rs. Using the potencies and the efficacies obtained from luciferase reporter gene- and the β-arrestin2 recruitment assays at the h/m/rH_4Rs, a bias analysis for **33**, **35**, **38**, **43**, **45**, **46**, **48**, and **49** (Figure S2 in the Supporting Information) was performed as described by van der Westhuizen et al.[38] based on the operational model of agonism,[39−43] using histamine **1** as a reference agonist. The bias analysis accounts for several assay-specific effects, such as the aforementioned signal amplification. Other effects, including cross-talks between different signaling influence the determined bias profile, too. Nevertheless, it can be taken as a hint at functionally selective signaling profiles of the investigated 2,4-diaminopyrimdines. Based on this analysis, **33**, **43**, **45**, **46**, **48**, and **49** showed a preference for the G-protein mediated pathway ($\Delta\Delta\log(\tau/K_A) > 0$) for at least one of the investigated receptor orthologs, whereas **35** and **38** were found to have a balanced bias profile ($\Delta\Delta\log(\tau/K_A) \approx 0$) (Figure S2 in the Supporting Information). Additionally, the 2,4-diaminopyrimidines with pK_i values < 7.0 at the hH_4R (**34**, **36**, **37**, **39**−**42**, **44**, **47**, and **50**−**52**) were screened for activity

DOI: 10.1021/acs.jmedchem.9b01342
J. Med. Chem. XXXX, XXX, XXX−XXX

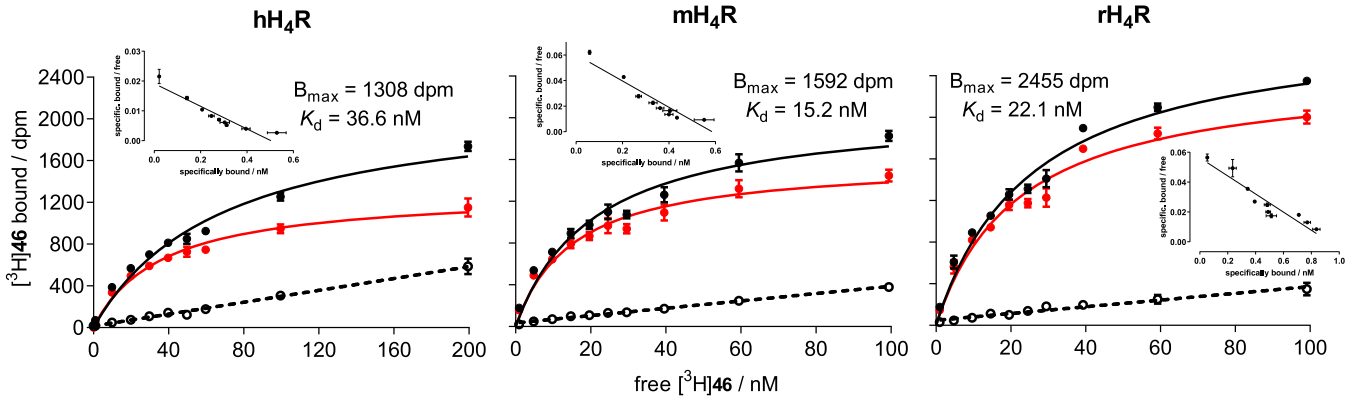

Figure 3. Representative data from saturation binding experiments at the hH_4R, mH_4R or rH_4R, coexpressed in homogenates of HEK293T-SF-His6-CRE-Luc cells. Total binding (black curve), specific binding (red curve), and nonspecific binding (dashed line, determined in the presence of **6** (1000-fold excess)) of [^{3}H]**46** are depicted. Insets: Scatchard transformations of shown specific binding curves. The experiments were performed in triplicate. Error bars of specific binding and in the Scatchard plots were calculated according to the Gaussian law of error propagation. Error bars of total and nonspecific binding represent SEMs.

Table 3. Comparison of Kinetic and Thermodynamic Binding Constants of [^{3}H]46 at the Human (h), Mouse (m), and Rat (r) H_4Rs

H_4R	K_d (sat)[a] [nM]	K_d (kin)[b] [nM]	k_{obs} [min^{-1}][c]	k_{on} [min^{-1}·nM^{-1}][d]	k_{off} [min^{-1}][e], $t_{1/2}$ [min][e]
h	41.3 ± 2.0	59 ± 18	0.19 ± 0.02	0.0019 ± 0.0005	0.113 ± 0.010, 6.2 ± 0.6
m	17.1 ± 0.8	34 ± 12	0.19 ± 0.02	0.0035 ± 0.0013	0.1204 ± 0.0093, 5.8 ± 0.4
r	21.8 ± 0.2	34 ± 6	0.205 ± 0.006	0.0032 ± 0.0005	0.11 ± 0.01, 6.6 ± 0.7

[a]Equilibrium dissociation constant determined by saturation binding on homogenates of HEK293T-SF-His6-CRE-Luc cells co-expressing the respective receptor; means ± SEM from at least three independent experiments each performed in triplicate. [b]Kinetically derived dissociation constant ± propagated error (K_d (kin) = k_{off}/k_{on}). [c]Observed association rate constant represents means ± SEM from two to three independent experiments each performed in triplicate at homogenates of HEK293T-SF-His6-CRE-Luc cells coexpressing the respective receptor. [d]Association rate constant ± propagated error ($k_{on} = (k_{obs} - k_{off})/[RL]$). [e]Dissociation rate constant and derived half-life represent means ± SEM from two to three independent experiments each performed in triplicate at homogenates of HEK293T-SF-His6-CRE-Luc cells co-expressing the respective receptor.

at the mH_4R and the rH_4R in the β-arrestin2 recruitment- and luciferase reporter gene assays applying three distinct concentrations (100 nM, 1 μM, 10 μM) for each compound in the agonist mode and antagonist mode ($\alpha < 0.1$) (Table S1 in the Supporting Information). For all investigated compounds, no indication for ortholog selectivity for the mH_4R or rH_4R was found.

In view of a radioligand for comparative binding studies at the h/m/rH_4Rs, three 2,4-diaminopyrimidines **43**, **45**, and **46** qualified as potential candidates, having high potencies (pEC_{50} > 7.0) and comparable efficacies across all analyzed H_4R orthologs in both functional assays. As a number of important requirements should be fulfilled for radiosynthesis, **43** and **45** were not considered for tritium labeling. First of all, the labeled moiety should be introduced in the last synthetic step under as mild and controllable reaction conditions as possible. The labeling reagent should be easy to handle and should not be too reactive. Moreover, according to the ALARA principle ("as low as reasonable achievable"; see Recommendation of the International Commission on Radiological Protection, e.g., IRCP Publication 26[44] and 103[45]), the reaction should lead to a high radiochemical yield and as little radioactive side-products and waste as possible. Finally, the "hot" compound should be easy to purify without the need for complex work-up procedures and too specialized equipment. Therefore, **46** (UR-DEBa176) was favored because of its convenient synthesis by controlled monomethylation of an excess of **45** with a tritium-labeled reagent (e.g., methyl nosylate [methyl-^{3}H] or methyl iodide [methyl-^{3}H]) (Figure 2).

Synthesis, Analytical Characterization, and Long-Term Stability of the Radiolabeled 2,4-Diaminopyrimidine [^{3}H]46. The tritium-labeled 2,4-diaminopyrimidine [^{3}H]**46** ([^{3}H]UR-DEBa176) was prepared by treating an excess of the methylamine precursor **45** with commercially available methyl nosylate [methyl-^{3}H] ([^{3}H]**53**) in the presence of K_2CO_3 at room temperature (Figure 2). Methyl nosylate [methyl-^{3}H] was favored over the commonly used volatile methyl iodine [methyl-^{3}H] due to technical reasons (handling, safety precautions). The desired radioligand [^{3}H]**46** ([^{3}H]UR-DEBa176) was isolated by reverse phase (RP)-HPLC in a radiochemical yield of 29% (108.5 MBq) and of a high radiochemical purity of 99%. The specific activity amounted to 1.59 TBq/mmol (43.08 Ci/mmol), and the final activity concentration was adjusted to 58.1 MBq/mL (1.6 mCi/mL). [^{3}H]**46** revealed a high chemical stability over a storage period of 11 months at −20 °C in EtOH/H_2O (70:30) (Figure 2).

Saturation Binding Experiments with [^{3}H]46 at the Human, Mouse, and Rat H_4Rs. Saturation binding experiments with [^{3}H]**46** were performed with homogenates of HEK293T-SF-His6-CRE-Luc cells coexpressing the hH_4R, mH_4R or rH_4R. Representative saturation binding curves and the corresponding Scatchard plots are depicted in Figure 3. [^{3}H]**46** bound to all H_4R orthologs in a saturable manner, revealing comparable K_d values at the h/m/rH_4Rs of 41.3 ± 2.0, 17.1 ± 0.8 and 21.8 ± 0.2 nM, respectively (Figure 3 and Table 3). The determined dissociation constants (K_d) for [^{3}H]**46** were in agreement with the pK_i or pEC_{50} values obtained in the competition binding assay (hH_4R) or in the β-arrestin2

DOI: 10.1021/acs.jmedchem.9b01342
J. Med. Chem. XXXX, XXX, XXX−XXX

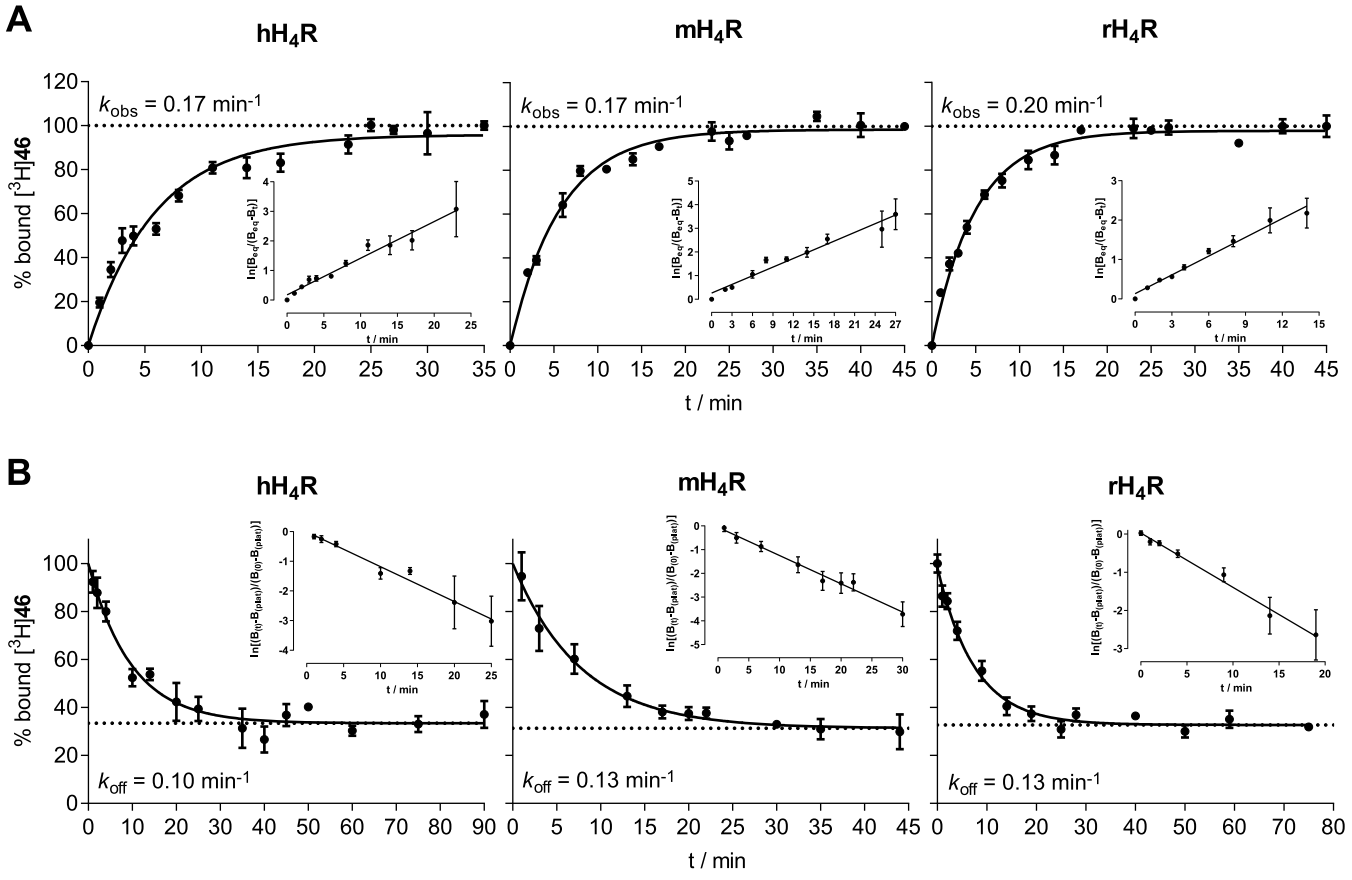

Figure 4. Comparison of the kinetic binding experiments with [^{3}H]**46** at the hH$_4$R, mH$_4$R or rH$_4$R, co-expressed in homogenates of HEK293T-SF-His6-CRE-Luc cells. (A) Representative associations of [^{3}H]**46** (c = 40 nM, hH$_4$R; 20 nM, mH$_4$R; 30 nM, rH$_4$R) as a function of time (k_{obs}, observed association rate constant). Insets: Transformation of the depicted association kinetics using $\ln[B_{(eq)}/(B_{(eq)} - B_{(t)})]$ versus time. (B) Representative dissociation of [^{3}H]**46** (preincubation: 30−45 min, c = 40 nM, hH$_4$R; 20 nM, mH$_4$R; 30 nM, rH$_4$R) in the presence of **6** (1000-fold excess) as a function of time (k_{off}, dissociation rate constant), showing an incomplete monophasic exponential decline [plateau: 33.4% (hH$_4$R), 31.3% (mH$_4$R), 33.5% (rH$_4$R)]. Insets: transformation of the depicted dissociation kinetics using $\ln[(B_{(t)} - B_{(plateau)})/(B_{(0)} - B_{(plateau)})]$ vs time. Each experiment was performed in triplicates. Error bars represent propagated errors according to the Gaussian law of error.

Table 4. Comparison of the Determined Binding Data (pK_i) of Unlabeled hH$_4$R Ligands (1, 4, 5, and 6), Using[^{3}H]46 as Radioligand at the H$_4$R Orthologs, to Reference Data

	pK_I/pEC$_{50}$ or pK_b /(α)					
	hH$_4$R		mH$_4$R		rH$_4$R	
no.	[^{3}H]**46**[a]	reference[b]	[^{3}H]**46**[a]	reference[c,d,e,f]	[^{3}H]**46**[a]	reference[c,d,e,f]
1	**7.22 ± 0.07**	**7.8−8.2**[1−7]	**6.31 ± 0.06**	5.1−7.06 (1.0)	**5.71 ± 0.06**	4.3−6.5 (1.0)
4	**7.25 ± 0.07**	**7.6−8.4**[1,3−6]	**6.76 ± 0.06**	6.1 (0.2)[c] 6.7 (0.6)[f]	**6.57 ± 0.04**	6.3 (0.0)[c] 6.8 (0.4)[f]
5	**7.30 ± 0.09**	**7.2−8.4**[1−3,5,7]	**6.94 ± 0.05**	6.1−6.9, 7.6 (−0.2−0.6)	**6.91 ± 0.10**	6.1−8.2 (0.2−0.5)
6	**6.45 ± 0.07**	**6.3−7.3**[1−3,6,7]	**7.13 ± 0.05**	6.5, 7.1−7.6 (−0.4−0.0)	**6.56 ± 0.03**	5.9−6.9 (−0.2−0.0)

[a]Data from competition binding experiments (pK_i) with [^{3}H]**46** (40 nM, hH$_4$R; 20 nM, mH$_4$R; 30 nM, rH$_4$R) for hH$_4$R standard ligands, determined at the human, mouse, or rat H$_4$Rs, co-expressed in homogenates of HEK293T-SF-His6-CRE-Luc cells. The pK_i values represent means ± SEM and were determined in at least three independent experiments, each performed in triplicate. [b]Data from competition binding experiments (pK_i) with [1][^{3}H]**2** or [2−7][^{3}H]**1**, performed on [1]membrane preparations of *Sf*9 insect cells, stably expressing the hH$_4$R-RGS19 fusion protein + Gα_{i2} + G$\beta_1\gamma_2$,[12] [2]membrane preparations of *Sf*9 insect cells, stably expressing the hH$_4$R-RGS19 fusion protein + Gα_i + G$\beta_1\gamma_2$,[16] [3]membrane preparations of *Sf*9 insect cells, stably expressing the hH$_4$R + Gα_{i2} + G$\beta_1\gamma_2$,[17,34,50] [4]homogenates of SK-N-MC-cells, stably expressing the hH$_4$R,[14] [5]membranes from SK-*N*-MC cells, stably expressing the hH$_4$R,[3,23,51] [6]homogenates of HEK293T-cells, stably expressing the hH$_4$R[21,24] or [7]HEK293T cells, stably expressing the hH$_4$R.[22] [c]Data from [^{35}S]GTPγS assays,[17] performed on membrane preparations of *Sf*9 insect cells, stably expressing the mH$_4$R or rH$_4$R + Gα_{i2} + G$\beta_1\gamma_2$. [d]Data from steady-state [^{32}P]GTPase assays,[16] performed on membrane preparations of *Sf*9 insect cells, stably expressing the mH$_4$R or rH$_4$R + Gα_{i2} + G$\beta_1\gamma_2$ + GAIP. [e]Data from β-arr2 recruitment assays in HEK293T cells, stably expressing the mH$_4$R or rH$_4$R-ELucC/ELucN-β-arrestin2 construct. [f]Data from CRE-luciferase reporter gene assays[26] in HEK293T cells, stably expressing the mH$_4$R or rH$_4$R with the CRE-controlled luciferase reporter gene.

recruitment assays (h/m/rH$_4$Rs) for the unlabeled **46** (Tables 1−3). The nonspecific binding is low, amounting 11−17% of total binding at concentrations around the K_d (Figure 3). The maximal number of binding sites (B_{max}) resulted in approx. 3.9 (hH$_4$R), 2.0 (mH$_4$R), and 2.9 (rH$_4$R) pmol·mg^{-1} soluble homogenate protein.

DOI: 10.1021/acs.jmedchem.9b01342
J. Med. Chem. XXXX, XXX, XXX−XXX

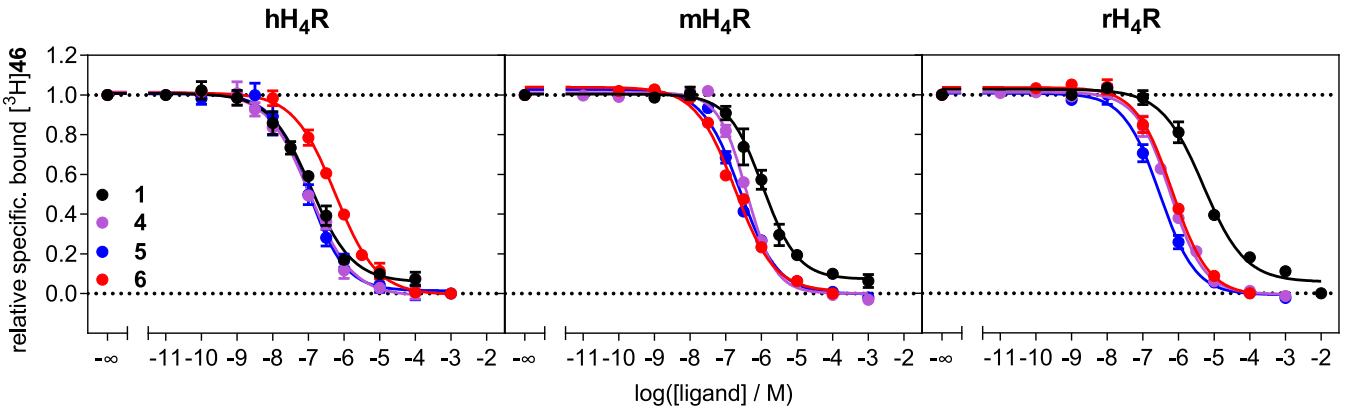

Figure 5. Radioligand displacement curves from competition binding experiments performed with [^{3}H]**46** (40 nM, hH$_4$R; 20 nM, mH$_4$R; 30 nM, rH$_4$R) at the hH$_4$R, mH$_4$R, or rH$_4$R, coexpressed in homogenates of HEK293T-SF-His6-CRE-Luc cells. Data represent mean values ± SEM of at least three independent experiments, each performed in triplicate.

Kinetic Binding Experiments with [^{3}H]46 at the Human, Mouse, and Rat H$_4$Rs. Kinetic binding experiments with [^{3}H]**46** were performed with homogenates of HEK293T-SF-His6-CRE-Luc cells coexpressing the hH$_4$R, mH$_4$R, or rH$_4$R. Representative nonlinear and linear plots for the association and dissociation of [^{3}H]**46** are shown in Figure 4. Association was complete after 25 minutes for all three H$_4$R orthologs. After 30 minutes, the residual specific binding of [^{3}H]**46** reached approx. 30% at the h/m/rH$_4$Rs, which might be partly explained by (pseudo)irreversible binding. This phenomenon was observed before, with respect to radioligands for several GPCRs.[28,46−48] Nonetheless, the kinetically derived dissociation constants [K_d (nM) = k_{off}/k_{on} = 59 ± 18 (hH$_4$R), 34 ± 12 (mH$_4$R) and 34 ± 6 (rH$_4$R)] were in a good agreement with the K_d values obtained from saturation binding experiments (Table 3).

Competition Binding Experiments with [^{3}H]46 for 1 and 4−6 at the Human, Mouse, and Rat H$_4$Rs. Competition binding experiments with [^{3}H]**46** and with several standard ligands (**1** and **4**−**6**) for the hH$_4$R were performed with homogenates of HEK293T-SF-His6-CRE-Luc cells co-expressing the hH$_4$R, mH$_4$R, or rH$_4$R (Table 4 and Figure 5). At the hH$_4$R, the pK_i values of the inverse agonists/antagonists (**5** and **6**) were in good agreement with the published data. In contrast, for the investigated agonists (**1** and **4**), slightly lower affinities were observed for the hH$_4$R in comparison to the literature, most distinctive for histamine **1**, with 0.8 orders of magnitude. These discrepancies might reflect the different efficacies of the radioligands used. While [^{3}H]**46** appeared as a partial agonist, the standard hH$_4$R radioligands [^{3}H]**1** or [^{3}H]**2** reveal full agonistic activities.[26] In this context, the unknown and varying G-protein expression levels in the different assay systems can carry weight as well. A report on competition binding studies at the 5-HT$_{2A}$ receptor[49] supports this hypothesis, showing that the affinities of agonists depend on the intrinsic efficacy of the used radioligand. Nonetheless, the affinities of all analyzed standard ligands at the mH$_4$R and rH$_4$R fit in the ranges defined by their pEC$_{50}$ and/or the pK_b values, derived from different functional assays with different signal readouts (Table 4). Therefore, [^{3}H]**46** allows comparative binding studies at the h/m/rH$_4$Rs.

CONCLUSIONS

Here, we report on the development of the 2,4 diaminopyrimidine-type radioligand [^{3}H]UR-DEBa176 ([^{3}H]**46**), enabling robust comparative binding studies at the h/m/rH$_4$Rs [K_d = 41, 17, 22 nM, respectively; low non-specific binding (11−17%, ~K_d); fast association/dissociation kinetics (25−30 min)]. Therefore, extensive investigations on the prepared 2,4-diaminopyrimidines with respect to their affinities at the hH$_4$R and their functional profiles at the h/m/rH$_4$Rs in different assays (luciferase reporter gene-, β-arrestin2 recruitment assays) were conducted. On the one hand, **43** (UR-DEBa148) was found to exhibit sub-nanomolar potencies at the h/m/rH$_4$Rs in luciferase reporter gene assays (pEC$_{50}$ = 9.9, 9.6, 10.3, respectively) and was slightly G-protein biased. On the other hand, (partial) agonist **46** (UR-DEBa176), with comparable potencies at the h/m/rH$_4$Rs [pEC$_{50}$ (reporter gene) = 8.7, 9.0, 9.2, respectively], was found to constitute the "cold" form of a potential radioligand. Subsequently, by employing commercially available methyl nosylate [methyl-^{3}H] ([^{3}H]**53**), [^{3}H]UR-DEBa176 ([^{3}H]**46**) was obtained in a radiochemical yield of 29% and of a high radiochemical purity of 99%. As a molecular tool, [^{3}H]UR-DEBa176 ([^{3}H]**46**) allows pharmacological investigations on the H$_4$R with respect to translational animal models (e.g., early stage characterization of novel molecular tools or potential drug candidates in radioligand binding assays at the h/m/rH$_4$Rs). To conclude, the herein presented SAR results and especially [^{3}H]UR-DEBa176 ([^{3}H]**46**) should support the future development of h/m/rH$_4$Rs ligands and can help to further unravel the (patho)physiological role of the H$_4$R.

EXPERIMENTAL SECTION

General Experimental Conditions. Chemicals and solvents were purchased from Acros Organics (Geel, Belgium), Alfa Aesar & Co. KG (Karlsruhe, Germany), Sigma-Aldrich (Munich, Germany), TCI (Tokyo, Japan), Tocris (Wiesbaden-Nordenstadt, Germany), and Merck KGaA (Darmstadt, Germany) and were used without further purification. All solvents were purchased in analytical degrade or distilled prior to use and stored over molecular sieves (4 Å). Acetonitrile (MeCN) (gradient grade) for HPLC was obtained from Merck (Darmstadt, Germany). Millipore water was used for the preparation of HPLC eluents. Deuterated solvents for NMR spectroscopy were from Deutero GmbH (Kastellaun, Germany). For column chromatography, Merck silica gel 60 (0.040−0.063 mm) was used. Flash chromatography was performed on an Intelli Flash-310 Flash-Chromatography Workstation from Varian Deutschland

DOI: 10.1021/acs.jmedchem.9b01342
J. Med. Chem. XXXX, XXX, XXX−XXX

GmbH (Darmstadt, Germany). Reaction controls were performed using thin layer chromatography (TLC) on Merck silica gel 60 F_{254} TLC aluminium sheets [visualization either by UV radiation (λ = 254 or 310 nm) or staining with ninhydrine or vanillin, respectively]. For microwave-driven reactions, a Biotage Initiator microwave synthesizer (Biotage, Uppsala, Sweden) was used. NMR spectra were recorded on a Bruker AVANCE 300 (7.05 T, ^{1}H 300 MHz; ^{13}C 75 MHz), Bruker Avance III HD 400 (9.40 T, ^{1}H 400 MHz; ^{13}C 101 MHz), or Bruker Avance III HD 600, equipped with a cryogenic probe (14.1 T, ^{1}H 600 MHz; ^{13}C 151 MHz) (Bruker BioSpin, Karlsruhe, Germany) with tetramethylsilane as an external standard. Multiplicities are specified with the following abbreviations: s (singlet), d (doublet), t (triplet), q (quartet), m (multiplet), br (broad signal), and quat. (quaternary carbon atom). The coupling constants (J values) are given in hertz (Hz). High-resolution mass spectrometry (HRMS) analysis was performed on an Agilent 6540 UHD Accurate-Mass Q-TOF LC/MS system (Agilent Technologies, Santa Clara, CA) using an ESI (electrospray ionization) source. Melting points were determined (if applicable) on a Büchi 530 (Büchi GmbH, Essen, Germany) and were uncorrected. Preparative HPLC was performed on a Knauer device (Berlin, Germany), comprising two K-1800 pumps and a K-2001 detector. An Interchim puriFlash C18 HQ 15 UM (120G Flash COLUMN 15 μm) with a flow rate of 50 mL/min or a Phenomenex Kinetex 5u XB-C18 (250 × 21.2 mm) with a flow rate of 15 or 20 mL/min was used as stationary phases. Mixtures of 0.1% TFA (B) and MeCN (A) served as the mobile phase. The detection wavelength was set to 220 nm. All compound solutions were filtered through polytetrafluoroethylene (PTFE) filters (25 mm, 0.2 μm, Phenomenex Ltd., Aschaffenburg, Germany) prior to injection. The solvent of the collected fractions was removed under reduced pressure followed by lyophilization using an Alpha 2-4 LD apparatus (Martin Christ, Osterode am Harz, Germany) equipped with a RZ 6 rotary vane vacuum pump (Vacuubrand, Wertheim, Germany). For all target compounds, 10 mM stock solutions in dimethyl sulfoxide (DMSO)/20 mM HCl 1/1 (v/v) were prepared in polypropylene reaction vessels (1.5 mL) with a screw cap (Süd-Laborbearf, Gauting, Germany). Analytical HPLC analysis (purity control and determination of the chemical stability of compounds) was performed with a system from Agilent Technologies (Series 1100) composed of a binary pump equipped with a degasser (G1312A), autosampler (ALS, G1329A), thermostated column compartment (COLCOM, G1316A), and diode array detector (DAD, G1315B). A Phenomenex Kinetex-XB C18 (2.6 μm, 100 mm × 3 mm) was used as a stationary phase at a flow rate of 0.8 mL/min. Mixtures of 0.5% TFA (A) and MeCN + 0.5% TFA (B) served as a mobile phase. The following linear gradient was applied throughout: A/B (v/v) 0−30 min, 90/10−10/90; 30−33 min, 10/90−5/95; 33−40 min, 5/95. For all analytical runs, the oven temperature was set to 30 °C, and detection was performed at 220 nm. The injection volume for purity controls was 60 μL of a 100 μM solution (10 mM stock solution diluted with starting eluent, A/B 90/10). Retention (capacity) factor (k) was calculated based on the determined retention time (t_R) according to $k = (t_R - t_0)/t_0$ (t_0 = dwell time = 3.21 min).

Compound Characterization. The synthesized compounds **8**, **9**, **11**−**15**, **20**−**52**, **61**, and **63**−**67** were characterized by ^{1}H and ^{13}C NMR spectroscopy, HRMS, and melting point (if applicable) (^{1}H, ^{13}C NMR spectra for selected target structures see Figures S3−S22 in the Supporting Information). Additionally, compounds **8**, **9**, **11**−**13**, **15**, **20**−**52**, **61**, **63**, and **65**−**67** were characterized by 2D-NMR spectroscopy (^{1}H-COSY, HSQC, HMBC). The intermediate compounds 7 and **10** were characterized by ^{1}H NMR spectroscopy, HRMS, and melting point (if applicable). The purity of the target compounds (**33**−**52**) was >96% throughout, determined by RP-HPLC (220 nm) (conditions see General Experimental Conditions; chromatograms see Figures S23−S32 in the Supporting Information).

The comment regarding the NMR spectra (^{1}H, ^{13}C) of the target 2,4-diaminpyrimidines, substituted with unsymmetrical cyclic aliphatic amines in the 4-position (**33**, **35**, **43**, **45**, **46**, **48**, **49**, **51**, and **52**) is the following: the slow rotation around the amine bond on the NMR time scale resulted in two isomers (ratios are given in the experimental protocols), which were evident in the ^{1}H- and ^{13}C NMR spectra.

Screening for Pan-Assay Interference Compounds (PAINS). The screening of the target compounds for PAINS and aggregators by the public tool http://zinc15.docking.org/patterns/home,[32] led to no hits except for compound **44**. Here, the 4-[(ethylthio)methyl]-1*H*-imidazole substructure was identified as PAIN. The identity of **44** was proven by HRMS, ^{1}H- and ^{13}C NMR spectroscopy. Additionally, analytical RP-HPLC revealed a purity of 98.9% (conditions see General Experimental Conditions). **44** showed only weak to no affinities at the human $H_{1\text{-}4}$Rs, while dose−response curves were measured in radioligand competition binding assays. Moreover, the amine precursor for **44**, 2-{[(5-methyl-1*H*-imidazole-4yl)methyl]-thio}ethan-1-amine, exhibits only weak agonistic activity at the human $H_{3,4}$Rs in the [^{35}S]GTPγS assay as well.[34] Therefore, an interference in the applied pharmacological assays by an impurity, containing the 4-[(ethylthio)methyl]-1*H*-imidazole scaffold, can be excluded.

Synthesis of the Target Compounds. *General Procedure for **33**−**43**.* The respective 4-amino-2-chloropyrimidine (1 equiv), DIPEA (1.5−6 equiv), and 2,2-dimethylpropan-1-amine (2−6 equiv) were dissolved in *i*-PrOH. The reaction mixture was stirred in the microwave reactor for 4−11 h at 120−140 °C. After removing the solvent under reduced pressure, the product was purified by chromatography or automated flash-chromatography. The residue was dissolved in dichloromethane (DCM), TFA was added, and the mixture was stirred at rt until the removal of the protection group was complete (7−18 h). The crude product was purified by preparative HPLC.

*(R)-4-(3-Aminopyrrolidin-1-yl)-N-neopentylpyrimidin-2-amine Bis(2,2,2-trifluoroacetate) **33**.*[29] According to the general procedure, the title compound was prepared in the microwave reactor (6 h, 130 °C, 4 bar, 3 min prestirring) from **20** (400 mg, 1.34 mmol), DIPEA (456 μL, 2.68 mmol), and 2,2-dimethylpropan-1-amine (475 μL, 3.87 mmol) in *i*-PrOH (4 mL). The crude product was purified by chromatography [eluent: DCM/MeOH 100/0−95/5 (v/v), SiO_2 50 g] to give **32** as pale, yellow sticky foam (450 mg, 96.2%). R_f = 0.45 (DCM/MeOH 92.5/7.5). ^{1}H NMR (400 MHz, DMSO-d_6): δ (ppm) 7.72 (d, J = 5.8 Hz, 1H), 7.18 (br, 1H), 6.43 (br, 1H), 5.67 (d, J = 5.8 Hz, 1H), 4.22−3.07 (m, 7H), 2.20−1.73 (m, 2H), 1.39 (s, 9H), 0.87 (s, 9H). ^{13}C NMR (101 MHz, DMSO-d_6, HSQC, HMBC): δ (ppm) 162.56 (quat., 1C), 160.61 (quat., 1C), 155.71, 155.44 (quat., 1C), 93.77, 78.31 (quat., 1C), 52.00, 51.84, 50.17, 44.53, 32.85, 30.76, 28.68 (3C), 27.99 (3C). HRMS (ESI) m/z: [M + H]$^+$ calcd for $[C_{18}H_{32}N_5O_2]^+$, 350.2551; found, 350.2564. $C_{18}H_{31}N_5O_2$ (349.48). Deprotection of **32** (140 mg, 0.401 mmol) in DCM (4 mL) and TFA (0.6 mL) followed by preparative HPLC [Interchim puriFlash C18 HQ 15 UM 120G Flash COLUMN 15 μm; gradient 0−30 min: A/B (v/v) 95/5−38/62, t_R = 9.5 min] afforded **33** as colorless hygroscopic foam (150 mg, 78.4%). R_f = 0.3 (DCM/1.75 M NH_3 in MeOH 90/10). RP-HPLC (220 nm): 99.9% (k = 1.81). Ratio of configurational isomers evident in NMR: ca. 1:1.4. ^{1}H NMR (600 MHz, DMSO-d_6): δ (ppm) 12.47 (br, 1H), 8.43 (m, 1H), 8.22 (m, 3H), 7.88 (m, 1H), 6.21 (d, J = 7.0 Hz, 1H), 4.10−3.49 (m, 5H), 3.22 (m, 2H), 2.41−2.01 (m, 2H), 0.90 (s, 9H). ^{13}C NMR (151 MHz, DMSO-d_6, HSQC, HMBC): δ (ppm) 159.54 (quat., 1C), 159.43 (quat., 1C), 158.55 (q, J = 33.0 Hz, TFA), 153.43, 142.51, 116.64 (q, J = 296.9 Hz, TFA), 95.44, 51.29, 50.51, 50.48, 49.45, 48.62, 45.02, 44.84, 32.26 (quat., 1C), 28.90, 28.18, 27.14 (3C). HRMS (ESI) m/z: [M + H]$^+$ calcd for $[C_{13}H_{24}N_5]^+$, 250.2026; found, 250.2033. $C_{13}H_{23}N_5\cdots C_4H_2F_6O_4$ (249.36 + 228.05).

*N-Neopentyl-4-(piperazin-1-yl)pyrimidin-2-amine Bis(2,2,2-trifluoroacetate) **34**.*[29] According to the general procedure, the title compound was prepared in the microwave reactor (7 h, 120 °C, 4 bar, 3 min prestirring) from **21** (800 mg, 2.70 mmol), DIPEA (917 μL, 5.39 mmol), and 2,2-dimethylpropan-1-amine (953 μL, 8.09 mmol) in *i*-PrOH (10 mL). The crude product was purified by chromatography (DCM/MeOH 100/0−95/5 (v/v), SiO_2 80 g) to give a colorless sticky foam (470 mg, 49.8%). R_f = 0.3 (DCM/MeOH 95/5). Deprotection (90 mg, 0.26 mmol) in DCM (2 mL) and TFA (0.5 mL) followed by preparative HPLC [column: Phenomenex

DOI: 10.1021/acs.jmedchem.9b01342
J. Med. Chem. XXXX, XXX, XXX−XXX

Kinetex 5u XB-C18 250 × 21.2 mm; gradient: 0−30 min: A/B (v/v) 95/5−43/57, flow 15 mL/min, t_R = 14 min] afforded **34** as colorless hygroscopic foam (112 mg, 91%). R_f = 0.4 (DCM/1.75 M NH_3 in MeOH 90/10). RP-HPLC (220 nm): 98.4% (k = 1.65). ^{1}H NMR (300 MHz, MeOH-d_4): δ (ppm) 7.80 (d, J = 7.5 Hz, 1H), 6.50 (d, J = 7.5 Hz, 1H), 4.16 (m, 4H), 3.40 (m, 6H), 0.98 (s, 9H). ^{1}H NMR (600 MHz, DMSO-d_6): δ (ppm) 12.92 (br, 1H), 9.26 (br, 2H), 8.56 (s, 1H), 7.97 (d, J = 7.4 Hz, 1H), 6.52 (d, J = 7.4 Hz, 1H), 3.96 (m, 4H), 3.23 (m, 6H), 0.90 (s, 9H). ^{13}C NMR (151 MHz, DMSO-d_6, HSQC, HMBC): δ (ppm) 161.17 (quat., 1C), 158.89 (q, J = 32.4 Hz, TFA), 153.73 (quat., 1C), 143.67, 116.83 (q, J = 297.5 Hz, TFA), 94.28, 51.36, 42.21 (2C), 40.04 (2C), 32.26 (quat., 1C), 27.10 (3C). HRMS (ESI) m/z: $[M + H]^+$ calcd for $[C_{13}H_{24}N_5]^+$, 250.2026; found, 250.2029. $C_{13}H_{23}N_5\cdots C_4H_2F_6O_4$ (249.36 + 228.05).

4-(1,4-Diazepan-1-yl)-N-neopentylpyrimidin-2-amine Bis(2,2,2-trifluoroacetate) ***35***.[29] According to the general procedure, the title compound was prepared in the microwave reactor (5.5 h, 130 °C, 3 bar, 3 min prestirring) from **22** (110 mg, 0.352 mmol), DIPEA (120 μL, 0.689 mmol), and 2,2-dimethylpropan-1-amine (83 μL, 0.70 mmol) in i-PrOH (2 mL). The crude product was purified by automated flash chromatography [gradient 0−20 min: DCM/MeOH 100/0−95/5 (v/v), SF 10−4 g] to give a colorless sticky foam (50 mg, 39.4%). R_f = 0.3 (DCM/MeOH 95/5). Deprotection (50 mg, 0.14 mmol) in DCM (2 mL) and TFA (0.3 mL) followed by preparative HPLC [column: Phenomenex Kinetex 5u XB-C18 250 × 21.2 mm; gradient: 0−30 min: A/B 95/5−33/67 (v/v), flow 20 mL/min, t_R = 11 min] afforded **35** as colorless hygroscopic foam (34 mg, 50.7%). R_f = 0.5 (DCM/1.75 M NH_3 in MeOH 80/20). RP-HPLC (220 nm): 97.5% (k = 1.86). Ratio of configurational isomers evident in NMR performed in DMSO-d_6: ca 1:1.5. ^{1}H NMR (400 MHz, MeOH-d_4): δ (ppm) 7.78 (d, J = 7.4 Hz, 1H), 6.46 (d, J = 6.9 Hz, 1H), 4.21 (t, J = 5.3 Hz, 1.3H), 4.04 (m, 1.4H), 3.81 (t, J = 6.1 Hz, 1.3 H), 3.50−3.31 (m, 6H), 2.20 (m, 2H), 0.99 (s, 9H). ^{1}H NMR (600 MHz, DMSO-d_6): δ (ppm) 12.84 (br, 1H), 9.08 (m, 2H), 8.49 (m, 1H), 7.92 (m, 1H), 6.45 (m, 1H), 4.13−3.62 (m, 4H), 3.41−3.11 (m, 6H), 2.04 (m, 2H), 0.91 (s, 9H). ^{13}C NMR (151 MHz, DMSO-d_6, HSQC, HMBC): δ (ppm) 161.68 (quat., 1C), 158.84 (q, J = 32.2 Hz, TFA), 153.58 (quat., 1C), 153.49 (quat., 1C), 143.11, 143.01, 116.87 (q, J = 298.2 Hz, TFA), 94.61, 51.31, 46.85, 45.64, 44.35, 44.27, 44.23, 44.13, 43.10, 32.20, 32.14, 27.12 (3C), 24.42, 24.13. HRMS (ESI) m/z: $[M + H]^+$ calcd for $[C_{14}H_{26}N_5]^+$, 264.2183; found, 264.2183. $C_{14}H_{25}N_5\cdots C_4H_2F_6O_4$ (263.39 + 228.05).

4-[4-(2-Aminoethyl)piperazin-1-yl]-N-neopentylpyrimidin-2-amine Tris(2,2,2-trifluoroacetate) ***36***. According to the general procedure, the title compound was prepared in the microwave reactor (9 h, 120 °C, 1 bar, 3 min prestirring) from **23** (110 mg, 0.322 mmol), DIPEA (110 μL, 0.632 mmol), and 2,2-dimethylpropan-1-amine (114 μL, 0.974 mmol) in i-PrOH (2 mL). The crude product was purified by chromatography [DCM/MeOH 100/0−90/10 (v/v), SiO_2] to give a pale, yellow sticky foam (80 mg, 63.5%). R_f = 0.4 (DCM/MeOH 90/10). Deprotection (80 mg, 0.20 mmol) in DCM (4 mL) and TFA (0.7 mL) followed by preparative HPLC (column: Phenomenex Kinetex 5u XB-C18 250 × 21.2 mm; gradient: 0−30 min: A/B 90/10−24/76 (v/v), flow 15 mL/min, t_R = 10 min) afforded **36** as colorless hygroscopic foam (57 mg, 44.5%). RP-HPLC (220 nm): 99.9% (k = 1.55). ^{1}H NMR (300 MHz, MeOH-d_4): δ (ppm) 7.71 (d, J = 7.6, 1H), 6.44 (d, J = 7.6 Hz, 1H), 4.07 (m, 2H), 3.79 (m, 2H), 3.30−3.09 (m, 4H), 2.87−2.65 (m, 6H), 0.97 (s, 9H). ^{1}H NMR (600 MHz, DMSO-d_6): δ (ppm) 12.60 (br, 1H), 8.42 (br. 1H), 7.90 (m, 4.5H), 6.53 (d, J = 7.3 Hz, 1H), 3.86 (m, 4H), 3.24−2.63 (m, 10H), 0.90 (s, 9H). ^{13}C NMR (151 MHz, DMSO-d_6, HSQC, HMBC): δ (ppm) 160.69 (quat., 1C), 158.65 (q, J = 33.0 Hz, TFA), 153.62 (quat., 1C), 143.27, 116.64 (q, J = 296.2 Hz, TFA), 94.19, 53.32, 51.47, 51.32, 44.29, 42.19, 34.90 (2C), 32.28 (quat., 1C), 27.10 (3C). HRMS (ESI) m/z: $[M + H]^+$ calcd for $[C_{15}H_{29}N_6]^+$, 293.2448; found, 293.2451. $C_{15}H_{28}N_6\cdots C_6H_3F_9O_6$ (292.43 + 342.07).

N^4-(2-Aminoethyl)-N^2-neopentylpyrimidine-2,4-diamine Bis(2,2,2-trifluoroacetate) ***37***. According to the general procedure, the title compound was prepared in the microwave reactor (6 h, 120 °C, 1 bar, 3 min prestirring) from **24** (150 mg, 0.550 mmol), DIPEA (140.3 μL, 0.82 mmol), and 2,2-dimethylpropan-1-amine (194 μL, 1.65 mmol) in i-PrOH (2 mL). The crude product was purified by automated flash chromatography [gradient 0−20 min: DCM/MeOH 100/0−90/10 (v/v), SF 10−4 g)]to give a colorless sticky oil (160 mg, 90%). R_f = 0.45 (DCM/MeOH 90/10). Deprotection (120 mg, 0.371 mmol) in DCM (2.5 mL) and TFA (0.5 mL) followed by preparative HPLC [Phenomenex Kinetex 5u XB-C18 250 × 21.2 mm; gradient 0−30 min: A/B (v/v) 95/5−38/62; flow: 15 mL/min; t_R = 12.5 min] afforded **37** as colorless hygroscopic foam (120 mg, 71.7%). RP-HPLC (220 nm): 99.9% (k = 1.61). ^{1}H NMR (300 MHz, MeOH-d_4): δ (ppm) 7.62 (d, J = 7.3 Hz, 1H), 6.10 (d, J = 7.0 Hz, 1H), 3.77 (t, J = 6.0 Hz, 2H), 3.33 (m, 2H), 3.22 (t, J = 6.1 Hz, 2H), 0.99 (s, 9H). ^{1}H NMR (600 MHz, DMSO-d_6): δ (ppm) 12.31 (br, 1H), 8.98 (s, 1H), 8.40 (s, 1H), 7.99 (br, 3H), 7.73 (d, J = 7.0 Hz, 1H), 6.04 (d, J = 7.0 Hz, 1H), 3.61 (m, 2H), 3.23 (m, 2H), 3.03 (m, 2H), 0.90 (s, 9H). ^{13}C NMR (151 MHz, DMSO-d_6, HSQC, HMBC): δ (ppm) 162.84 (quat., 1C), 158.71 (q, J = 32.3 Hz, TFA), 154.32 (quat., 1C), 141.45, 116.89 (q, J = 297.4 Hz, TFA), 97.42, 51.16, 37.99, 37.62, 32.16 (quat., 1C), 27.08 (3C). HRMS (ESI) m/z: $[M + H]^+$ calcd for $[C_{11}H_{22}N_5]^+$, 224.1870; found, 224.1874. $C_{11}H_{21}N_5\cdots C_4H_2F_6O_4$ (223.32 + 228.05).

N^4-(3-Aminopropyl)-N^2-neopentylpyrimidine-2,4-diamine Bis(2,2,2-trifluoroacetate) ***38***. According to the general procedure, the title compound was prepared in the microwave reactor (7 h, 120 °C, 2 bar, 3 min prestirring) from **25** (250 mg, 0.872 mmol), DIPEA (222 μL, 1.27 mmol), and 2,2-dimethylpropan-1-amine (616 μL, 5.23 mmol) in i-PrOH (2 mL). The crude product was purified by automated flash chromatography [gradient 0−20 min: DCM/MeOH 100/0−95/5 (v/v), SF 10−4 g] to give a colorless sticky oil (200 mg, 68%). R_f = 0.4 (DCM/MeOH 90/10). Deprotection of (190 mg, 0.563 mmol) in DCM (2 mL) and TFA (0.5 mL) followed by preparative HPLC (column: Phenomenex Kinetex 5u XB-C18 250 × 21.2 mm; gradient: 0−30 min: A/B 92.2/7.8−49.450.6 (v/v), flow 20 mL/min, t_R = 11 min) afforded **38** as colorless hygroscopic foam (188 mg, 71.7%). RP-HPLC (220 nm): 99.9% (k = 1.80). ^{1}H NMR (300 MHz, MeOH-d_4): δ (ppm) 7.56 (d, J = 7.3 Hz, 1H), 6.05 (d, J = 7.2 Hz, 1H), 3.58 (t, J = 6.7 Hz, 2H), 3.01 (m, 2H), 1.99 (m, 2H), 0.98 (s, 9H). ^{1}H NMR (600 MHz, DMSO-d_6, HSQC, HMBC): δ (ppm) 12.05 (br, 1H), 8.90 (br, 1H), 8.23 (br, 1H), 7.82 (br, 3H), 7.69 (d, J = 7.0 Hz, 1H), 6.03 (d, J = 7.0 Hz, 1H), 3.43 (m, 2H), 3.22 (m, 2H), 2.85 (m, 2H), 1.81 (m, 2H), 0.91 (s, 9H). ^{13}C NMR (151 MHz, DMSO-d_6): δ (ppm) 162.28 (quat., 1C), 158.48 (q, J = 31.4 Hz, TFA), 154.27 (quat., 1C), 141.21, 117.06 (q, J = 299.2 Hz, TFA), 97.16, 51.21, 37.50, 36.83, 32.14 (quat., 1C), 27.12 (3C), 26.54. HRMS (ESI) m/z: $[M + H]^+$ calcd for $[C_{12}H_{24}N_5]^+$, 238.2026; found, 238.2032. $C_{12}H_{23}N_5\cdots C_4H_2F_6O_4$ (237.35 + 228.05).

N^2-Neopentyl-N^4-(pyrrolidin-3-yl)pyrimidine-2,4-diamine Bis(2,2,2-trifluoroacetate) ***39***. According to the general procedure, the title compound was prepared in the microwave reactor (8 h, 120 °C, 2 bar, 3 min prestirring) from **26** (200 mg, 0.669 mmol), DIPEA (180 μL, 1.06 mmol), and 2,2-dimethylpropan-1-amine (237 μL, 2.01 mmol) in i-PrOH (2 mL). The crude product was purified by chromatography [DCM/MeOH 100/0−90/10 (v/v), SiO_2 30 g] to give a pale yellow sticky oil (160 mg, 68.2%). R_f = 0.4 (DCM/MeOH 90/10). Deprotection (150 mg, 0.430 mmol) in DCM (2 mL) and TFA (0.5 mL) followed by preparative HPLC (column: Phenomenex Kinetex 5u XB-C18 250 × 21.2 mm; gradient: 0−30 min: A/B 90/10−52/48 (v/v), flow 20 mL/min, t_R = 10.5 min) afforded **39** as colorless hygroscopic foam (97 mg, 47.4%). RP-HPLC (220 nm): 99.9% (k = 1.73). ^{1}H NMR (300 MHz, MeOH-d_4): δ (ppm) 7.64 (d, J = 7.2 Hz, 1H), 6.10 (d, J = 7.2 Hz, 1H), 4.74 (m, 1H), 3.52 (m, 6H), 2.29 (m, 2H), 0.99 (s, 9H). ^{1}H NMR (600 MHz, DMSO-d_6): δ (ppm) 12.42 (br, 1H), 9.15 (br, 3H), 8.50 (m, 1H), 7.76 (d, J = 7.1 Hz, 1H), 6.06 (d, J = 7.1 Hz, 1H), 4.55 (m, 1H), 3.45 (m, 1H), 3.40−2.98 (m, 5H), 2.27 (m, 1H), 1.95 (m, 1H), 0.91 (s, 9H). ^{13}C NMR (151 MHz, DMSO-d_6, HSQC, HMBC): δ (ppm) 162.17 (quat., 1C), 158.76 (q, J = 32.0 Hz, TFA), 154.22 (quat., 1C), 141.82, 116.95 (d, J = 298.5 Hz, TFA), 97.10, 51.23, 49.90, 49.30, 43.80, 32.17 (quat., 1C), 29.49, 27.07 (3C). HRMS (ESI) m/z: $[M + H]^+$ calcd for

DOI: 10.1021/acs.jmedchem.9b01342
J. Med. Chem. XXXX, XXX, XXX−XXX

$[C_{13}H_{24}N_5]^+$, 250.2026; found, 250.2031. $C_{13}H_{23}N_5\cdots C_4H_2F_6O_4$ (249.36 + 228.05).

N^2-Neopentyl-N^4-(piperidin-4-yl)pyrimidine-2,4-diamine Bis-(2,2,2-trifluoroacetate) 40. According to the general procedure, the title compound was prepared in the microwave reactor (7 h, 120 °C, 2 bar, 3 min prestirring) from **27** (250 mg, 0.799 mmol), DIPEA (204 μL, 1.17 mmol), and 2,2-dimethylpropan-1-amine (282 μL, 2.39 mmol) in *i*-PrOH (2 mL). The crude product was purified by automated flash chromatography [gradient 0−20 min: DCM/MeOH 100/0−95/5 (v/v), SF 10−4 g] to give a colorless sticky oil (120 mg, 41.4%). R_f = 0.4 (DCM/MeOH 90/10). Deprotection (110 mg, 0.303 mmol) in DCM (2 mL) and TFA (0.5 mL) followed by preparative HPLC [column: Phenomenex Kinetex 5u XB-C18 250 × 21.2 mm; gradient: 0−30 min: A/B 90/10−48/52 (v/v), flow 20 mL/min, t_R = 10 min] afforded **40** as colorless hygroscopic foam (100 mg, 67.2%). RP-HPLC (220 nm): 99.9% (k = 1.76). ^{1}H NMR (300 MHz, MeOH-d_4): δ (ppm) 7.59 (d, J = 7.3 Hz, 1H), 6.06 (d, J = 7.3 Hz, 1H), 4.30 (m, 1H), 3.32 (m, 6H), 2.24 (m, 2H), 1.80 (m, 2H), 0.98 (s, 9H). ^{1}H NMR (600 MHz, DMSO-d_6): δ (ppm) 12.29 (br, 1H), 9.92 (d, J = 6.4 Hz, 1H), 8.81 (br, 1H), 8.63 (br, 1H), 8.41 (m, 1H), 7.71 (d, J = 7.1 Hz, 1H), 6.03 (d, J = 7.0 Hz, 1H), 4.13 (m, 1H), 3.32 (m, 2H), 3.22 (m, 2H), 3.06 (m, 2H), 2.03 (m, 2H), 1.66 (m, 2H), 0.90 (s, 9H). ^{13}C NMR (151 MHz, DMSO-d_6, HSQC, HMBC): δ (ppm) 161.67 (quat., 1C), 158.66 (q, J = 47.3 Hz, TFA), 154.32 (quat., 1C), 141.54, 117.06 (q, J = 298.6 Hz, TFA), 97.12, 51.15, 45.20, 41.72 (2C), 32.19 (quat., 1C), 27.52 (2C), 27.12 (3C). HRMS (ESI) m/z: $[M + H]^+$ calcd for $[C_{14}H_{26}N_5]^+$, 264.2183; found, 264.2185. $C_{14}H_{25}N_5\cdots C_4H_2F_6O_4$ (263.39 + 228.05).

N^4-[2-(1H-Imidazole-4-yl)ethyl]-N^2-neopentylpyrimidine-2,4-diamine Bis(2,2,2-trifluoroacetate) 41. According to the general procedure, the title compound was prepared in the microwave reactor (11 h, 130 °C, 4 bar, 3 min prestirring) from **28** (150 mg, 0.322 mmol), DIPEA (330 μL, 1.89 mmol), and 2,2-dimethylpropan-1-amine (230 μL, 1.95 mmol) in *i*-PrOH (2 mL). The crude product was purified by automated flash chromatography [gradient 0−20 min: DCM/MeOH 100/0−90/10 (v/v), SF 10−4 g)] to give a colorless sticky foam (65 mg, 40%). R_f = 0.4 (DCM/MeOH 90/10). Deprotection (60 mg, 0.12 mmol) in DCM (2 mL) and TFA (0.5 mL) followed by preparative HPLC [Phenomenex Kinetex 5u XB-C18 250 × 21.2 mm; gradient 0−30 min: A/B (v/v) 86.5/14.4−28.5/71.5; flow: 20 mL/min; t_R = 8 min] afforded **41** as colorless hygroscopic foam (21 mg, 36.0%). RP-HPLC (220 nm): 99.0% (k = 2.02). ^{1}H NMR (300 MHz, MeOH-d_4): δ (ppm) 8.84 (s, 1H), 7.56 (d, J = 7.2 Hz, 1H), 7.38 (s, 1H), 6.02 (d, J = 7.0 Hz, 1H), 3.80 (t, J = 6.5 Hz, 1H), 3.28 (m, 2H), 3.07 (t, J = 6.5 Hz, 1H), 0.97 (s, 9H). ^{1}H NMR (600 MHz, DMSO-d_6, +10 μL TFA): δ (ppm) 11.98 (br, 3H), 9.00 (s, 1H), 8.89 (m, 1H), 8.24 (m, 1H), 7.67 (m, 1H), 7.44 (s, 1H), 6.00 (d, J = 6.9 Hz, 1H), 3.66 (m, 2H), 3.19 (m, 2H), 2.94 (m, 2H), 0.89 (s, 9H). ^{13}C NMR (151 MHz, DMSO-d_6, +10 μL TFA, HSQC, HMBC): δ (ppm) 162.46 (quat., 1C), 158.49 (q, J = 37.4 Hz, TFA), 154.24 (quat., 1C), 141.33, 133.99, 130.64 (quat., 1C), 116.39, 115.42 (q, J = 291.6 Hz, TFA), 97.22, 51.24, 39.33, 32.12 (quat., 1C), 27.11 (3C), 23.60. HRMS (ESI) m/z: $[M + H]^+$ calcd for $[C_{14}H_{23}N_5]^+$, 275.1979; found, 275.1983. $C_{14}H_{22}N_5\cdots C_4H_2F_6O_4$ (274.37 + 228.05).

N^4-[3-(1H-Imidazole-4-yl)propyl]-N^2-neopentylpyrimidine-2,4-diamine Bis(2,2,2-trifluoroacetate) 42. According to the general procedure, the title compound was prepared in the microwave reactor (10 h, 130 °C, 3 bar, 3 min prestirring) from **29** (140 mg, 0.292 mmol), DIPEA (300 μL, 1.72 mmol), and 2,2-dimethylpropan-1-amine (206 μL, 1.75 mmol) in *i*-PrOH (2 mL). The crude product was purified by automated flash chromatography [gradient 0−20 min: DCM/MeOH 100/0−90/10 (v/v), SF 10−4 g)] to a colorless sticky foam (100 mg, 64.9%). R_f = 0.45 (DCM/MeOH 90/10). Deprotection (70 mg, 0.13 mmol) in DCM (2 mL) and TFA (0.5 mL) followed by preparative HPLC [Phenomenex Kinetex 5u XB-C18 250 × 21.2 mm; gradient 0−30 min: A/B (v/v) 90/10−33/67, flow: 20 mL/min; t_R = 10.5 min] afforded **42** as hygroscopic foam (35 mg, 51.4%). RP-HPLC (220 nm): 99.9% (k = 2.23). ^{1}H NMR (300 MHz, MeOH-d_4): δ (ppm) 8.82 (m, 1H), 7.55 (d, J = 7.3 Hz, 1H), 7.35 (s, 1H), 6.04 (d, J = 7.2 Hz, 1H), 3.56 (t, J = 6.8 Hz, 2H), 3.27 (m, 2H), 2.82 (t, J = 7.7 Hz, 2H), 2.02 (m, 2H), 0.96 (s, 9H). ^{1}H NMR (600 MHz, DMSO-d_6, +10 μL TFA): δ (ppm) 11.89 (br, 3H), 8.98 (m, 1H), 8.81 (m, 1H), 8.13 (m, 1H), 7.67 (m, 1H), 7.43 (s, 1H), 6.02 (d, J = 7.0 Hz, 1H), 3.40 (m, 2H), 3.15 (m, 2H), 2.69 (t, J = 7.5 Hz, 2H), 1.89 (m, 2H), 0.87 (s, 9H). ^{13}C NMR (151 MHz, DMSO-d_6, +10 μL TFA, HSQC, HMBC): δ (ppm) 162.32 (quat., 1C), 158.49 (q, J = 37.4 Hz, TFA), 154.26 (quat., 1C), 141.15, 133.89, 132.67 (quat., 1C), 115.63, 115.46 (q, J = 290.2 Hz, TFA), 97.19, 51.20, 39.20, 32.16 (quat., 1C), 27.11 (3C), 27.00, 21.41. HRMS (ESI) m/z: $[M + H]^+$ calcd for $[C_{15}H_{25}N_6]^+$, 289.2135; found, 289.2136. $C_{15}H_{24}N_6\cdots C_4H_2F_6O_4$ (288.40 + 228.05).

N-Neopentyl-4-(1,4,6,7-tetrahydro-5H-imidazo[4,5-c]pyridin-5-yl)pyrimidin-2-amine Bis(2,2,2-trifluoroacetate) 43. According to the general procedure, the title compound was prepared in the microwave reactor (7.5 h, 130 °C, 3 bar, 3 min prestirring) from **30** (200 mg, 0.418 mmol), DIPEA (220 μL, 1.26 mmol), and 2,2-dimethylpropan-1-amine (150 μL, 1.27 mmol) in *i*-PrOH (3 mL). The crude product was purified by automated flash chromatography [gradient 0−20 min: DCM/MeOH 100/0−90/10 (v/v), SF 10−4 g] to give a yellow sticky oil (160 mg, 72.7%). R_f = 0.3 (DCM/MeOH 90/10). Deprotection (75 mg, 0.14 mmol) in DCM (2 mL) and TFA (0.4 mL) followed by preparative HPLC [column: Phenomenex Kinetex 5u XB-C18 250 × 21.2 mm; gradient: 0−30 min: A/B (v/v) 95/5−33/67, flow 15 mL/min, t_R = 13.5 min] afforded **43** as colorless hygroscopic foam (30 mg, 41.1%). RP-HPLC (220 nm): 96.2% (k = 1.97). Ratio of configurational isomers evident in NMR performed in DMSO-d_6: ca. 1:1.1. ^{1}H NMR (300 MHz, MeOH-d_4): δ (ppm) 8.79 (s, 1H), 7.81 (d, J = 7.5 Hz, 1H), 6.57 (m, 1H), 4.69 (m, 2H), 4.21 (m, 2H), 3.34 (m, 2H), 2.94 (m, 2H), 0.99 (s, 9H). ^{1}H NMR (600 MHz, DMSO-d_6): δ (ppm) 13.96 (br, 2H), 8.86 (s, 1H), 8.47 (br, 1H), 7.97 (d, J = 7.3 Hz, 1H), 6.61 (m, 1H), 5.00−3.00 (1 proton (NH^+) presumably superimposed by H_2O), 4.91 (m, 2H), 4.12 (m, 2H), 3.24 (m, 2H), 2.83 (m, 2H), 0.91 (s, 9H). ^{13}C NMR (151 MHz, DMSO-d_6, HSQC, HMBC): δ (ppm) 161.79 (quat., 1C) 158.72 (q, J = 32.3 Hz, TFA), 153.65 (quat., 1C), 143.82, 133.68, 125.76 (quat., 1C), 124.13 (quat., 1C), 116.90 (q, J = 297.8 Hz, TFA), 94.47, 51.42, 42.96, 42.86, 40.04, 32.96 (quat., 1C), 27.09 (3C), 20.82, 20.76. HRMS (ESI) m/z: $[M + H]^+$ calcd for $[C_{15}H_{23}N_6]^+$, 287.1979; found, 287.1982. $C_{15}H_{22}N_6\cdots C_4H_2F_6O_4$ (286.38 + 228.05).

N^4-(2-{[(5-Methyl-1H-imidazole-4-yl)methyl]thio}ethyl)-N^2-neopentylpyrimidine-2,4-diamine Bis(2,2,2-trifluoroacetate) 44. The title compound was prepared in the microwave reactor (4 h, 120 °C, 3 bar, 3 min prestirring) from **31** (110 mg, 0.388 mmol), DIPEA (132 μL, 0.758 mmol), and 2,2-dimethylpropan-1-amine (137 μL, 1.16 mmol) in *i*-PrOH (3 mL). After the solvent was removed under reduced pressure and the residue was dissolved in DCM (5 mL), the organic phase was washed with H_2O (3 × 2 mL) and brine (5 mL), and dried over $MgSO_4$. The crude product was purified by chromatography [DCM/MeOH 100/0−92.5/7.5 (v/v), SiO_2 13 g] and preparative HPLC [column: Phenomenex Kinetex 5u XB-C18 250 × 21.2 mm; gradient: 0−30 min: A/B 85.5/14.5−52.2/47.8 (v/v), flow 15 mL/min, t_R = 14.5 min] to yield **44** as colorless hygroscopic foam (38 mg, 17.4%). RP-HPLC (220 nm): 98.9% (k = 2.55). ^{1}H NMR (300 MHz, MeOH-d_4): δ (ppm) 8.75 (s, 1H), 7.56 (d, J = 7.3 Hz, 1H), 6.05 (d, J = 7.2 Hz, 1H), 3.88 (s, 2H), 3.68 (t, J = 6.8 Hz, 2H), 2.77 (t, J = 6.8 Hz, 2H), 2.33 (s, 3H), 0.96 (s, 9H). ^{1}H NMR (600 MHz, DMSO-d_6): δ (ppm) 14.24 (br, 3H), 8.99 (m, 1H), 8.88 (s, 1H), 8.39 (m, 1H), 7.69 (d, J = 7.0 Hz, 1H), 6.05 (d, J = 7.0 Hz, 1H), 3.86 (s, 2H), 3.55 (m, 2H), 3.19 (m, 2H), 2.68 (t, J = 6.7 Hz, 2H), 2.24 (s, 3H), 0.98 (s, 9H). ^{13}C NMR (151 MHz, DMSO-d_6, HSQC, HMBC): δ (ppm) 162.32 (quat., 1C), 158.59 (q, J = 31.4 Hz, TFA), 154.29 (quat., 1C), 141.40, 133.03, 125.94 (quat., 1C), 125.71 (quat., 1C), 117, 07 (q, J = 299.9 Hz, TFA), 97.10, 51.22, 39.74, 32.11 (quat., 1C), 29.81, 27.07 (3C), 23.13, 8.57. HRMS (ESI) m/z: $[M + H]^+$ calcd for $[C_{16}H_{27}N_6S]^+$, 335.2012; found, 335.2017. $C_{16}H_{26}N_6$ S···$C_4H_2F_6O_4$ (334.49 + 228.05).

(R)-4-[3-(Methylamino)pyrrolidin-1-yl]-N-neopentylpyrimidin-2-amine Bis(2,2,2-trifluoroacetate) 45.[29] In an argon-flushed Schlenk flask, **32** (480 mg, 1.37 mmol) was dissolved in anhydrous THF (10

DOI: 10.1021/acs.jmedchem.9b01342
J. Med. Chem. XXXX, XXX, XXX−XXX

mL). $LiAlH_4$ (267 mg, 7.04 mmol) was added in portions, and the reaction was stirred at 70 °C for 7 h. The reaction was cooled to 0 °C, quenched with H_2O (3 mL), and extracted with DCM (3 × 30 mL). The organic phases were combined, washed with brine (50 mL) and dried over $MgSO_4$. The crude product was purified by chromatography [DCM/1% $NH_{3(aq)}$ in MeOH (isocratic): 90/15 (v/v), SiO_2 30 g] and preparative HPLC [column: Phenomenex Kinetex 5u XB-C18 250 × 21.2 mm; gradient: 0−30 min: A/B 90/10−38/62 (v/v), flow 20 mL/min, t_R = 9 min] to yield **45** as colorless hygroscopic foam (290 mg, 43%). RP-HPLC (220 nm): 99.8% (k = 1.88). Ratio of configurational isomers evident in NMR performed in DMSO-d_6: ca 1:1.5. ^{1}H NMR (300 MHz, MeOH-d_4): δ (ppm) 7.74 (d, J = 7.4 Hz, 1H), 6.22 (m, 1H), 3.88 (m, 5H), 3.47−3.20 (m, 2H), 2.80 (s, 3H), 2.41 (m, 2H), 0.98 (m, 9H). ^{1}H NMR (600 MHz, DMSO-d_6): δ (ppm) 12.83 (br, 1H), 9.18 (m, 2H), 8.52 (m, 1H), 7.90 (m, 1H), 6.20 (d, J = 6.9 Hz, 1H), 3.97−3.56 (m, 5H), 3.23 (m, 2H), 2.64 (s, 3H), 2.42−2.12 (m, 2H), 0.90 (s, 9H). ^{13}C NMR (151 MHz, DMSO-d_6, HSQC, HMBC): δ (ppm) 159.57 (quat., 1C), 159.46 (quat., 1C), 158.97 (q, J = 32.6 Hz, TFA), 153.55 (quat., 1C), 143.53, 116.78 (q, J = 297.1 Hz, TFA), 95.44, 95.33, 57.34, 56.53, 51.30, 49.11, 48.79, 45.02, 44.85, 32.27 (quat., 1C), 31.22, 31.07, 27.13 (3C), 27.01, 26.66. HRMS (ESI) m/z: $[M + H]^+$ calcd for $[C_{14}H_{26}N_5]^+$, 264.2183; found, 264.2182. $C_{14}H_{25}N_5\cdots C_4H_2F_6O_4$ (263.39 + 228.05).

*General Procedure for **46**−**48**.* The respective 2,4-diaminopyrimidine bis(hydrotrifluoroacetate) (**33**−**35**) was dissolved in formic acid/formamide (1/1 v/v, 1.6 mL) and stirred at 95 °C until conversion was complete. Subsequently, the reaction mixture was quenched with saturated $NaHCO_{3(aq)}$ and extracted with EtOAc. The organic phases were combined, washed with brine, and dried over $MgSO_4$. After the solvent was removed under reduced pressure, the product was purified by preparative HPLC.

*(R)-4-[3-(Dimethylamino)pyrrolidin-1-yl]-N-neopentylpyrimidin-2-amine Bis(2,2,2-trifluoroacetate) **46**.* According to the general procedure, the title compound was prepared from **33** (150 mg, 0.312 mmol) at 95 °C over 5 h. The reaction mixture was quenched with saturated $NaHCO_{3(aq)}$ (7 mL) and extracted with EtOAc (2 × 100 mL). The organic phases were combined, washed with brine (100 mL), and dried over $MgSO_4$. After removing the solvent under reduced pressure, the product was purified by preparative HPLC [column: Phenomenex Kinetex 5u XB-C18 250 × 21.2 mm; gradient: 0−30 min: A/B 90/10−43/67 (v/v), flow 15 mL/min, t_R = 12 min] to yield **46** as colorless hygroscopic foam (90 mg, 56.6%). R_f = 0.4 (DCM/1.75 M NH_3 in MeOH 90/10). RP-HPLC (220 nm): 99.3% (k = 1.89). Ratio of configurational isomers evident in NMR performed in DMSO-d_6: ca 1:1.5. ^{1}H NMR (300 MHz, MeOH-d_4): δ (ppm) 7.74 (m, 1H), 6.22 (m, 1H), 3.94 (m, 5H), 3.30 (m, 2H), 2.99 (m, 6H), 2.46 (m, 2H), 0.98 (m, 2H). ^{1}H NMR (600 MHz, DMSO-d_6): δ (ppm) 12.50 (br, 1H), 10.54 (br, 1H), 8.35 (br, 1H), 7.92 (m, 1H), 6.22 (m, 1H), 4.00 (m, 2H), 3.87 (m, 0.6H), 3.74 (m, 1.6H), 3.55 (m, 1H), 3.25 (m, 1.8H), 2.85 (s, 6H), 2.29 (m, 2H), 0.90 (m, 9H). ^{13}C NMR (151 MHz, DMSO-d_6, HSQC, HMBC): δ (ppm) 159.50 (quat., 1C), 159.41 (quat., 1C), 158.62 (q, J = 32.2 Hz, TFA), 153.47 (quat., 1C), 142.70, 116.87 (q, J = 298.1 Hz, TFA), 95.37, 95.18, 63.76, 63.00, 51.30, 51.24, 47.92, 47.78, 45.60, 45.52, 41.50 (2C), 32.30 (quat 1C), 32.23 (quat., 1C), 27.14 (3C), 26.02, 25.86. HRMS (ESI) m/z: $[M + H]^+$ calcd for $[C_{15}H_{28}N_5]^+$, 278.2339; found, 278.2342. $C_{15}H_{27}N_5\cdots C_4H_2F_6O_4$ (277.42 + 228.05).

*4-(4-Methylpiperazin-1-yl)-N-neopentylpyrimidin-2-amine Bis-(2,2,2-trifluoroacetate) **47**.*[29] According to the general procedure, the title compound was prepared from **34** (150 mg, 0.314 mmol) over 5 h. The reaction mixture was quenched with saturated $NaHCO_{3(aq)}$ (7 mL) and extracted with EtOAc (2 × 100 mL). The organic phases were combined, washed with brine (100 mL), and dried over $MgSO_4$. After removing the solvent under reduced pressure, the product was purified by preparative HPLC [column: Phenomenex Kinetex 5u XB-C18 250 × 21.2 mm; gradient: 0−30 min: A/B 95/5−43/57 (v/v), flow 15 mL/min, t_R = 13.5 min] to yield **47** as colorless hygroscopic foam (75 mg, 48.7%). R_f = 0.6 (DCM/1.75 M NH_3 in MeOH 90/10). RP-HPLC (220 nm): 98.7% (k = 1.67). ^{1}H NMR (300 MHz, MeOH-d_4): δ (ppm) 7.82 (d, J = 7.5 Hz, 1H), 6.52 (d, J = 7.4 Hz, 1H), 4.71−3.31 (m, 10H), 2.96 (s, 3H), 0.98 (s, 9H). ^{1}H NMR (600 MHz, DMSO-d_6): δ (ppm) 12.84 (br, 1H), 10.67 (br, 1H), 8.57 (br, 1H), 7.99 (d, J = 7.3 Hz, 1H), 6.54 (d, J = 7.4 Hz, 1H), 5.26−3.02 (m, 10H), 2.82 (s, 3H), 0.90 (s, 9H). ^{13}C NMR (151 MHz, DMSO-d_6, HSQC, HMBC): δ (ppm) 161.19 (quat., 1C), 158.83 (q, J = 32.4 Hz, TFA), 153.76 (quat., 1C), 143.92, 116.89 (q, J = 298.6 Hz, TFA), 94.25, 51.67, 51.33 (2C), 42.10, 39.92 (2C), 32.29 (quat., 1C), 27.09 (3C). HRMS (ESI) m/z: $[M + H]^+$ calcd for $[C_{14}H_{26}N_5]^+$, 264.2183; found, 264.2184. $C_{14}H_{25}N_5\cdots C_4H_2F_6O_4$ (263.39 + 228.05).

*4-(4-Methyl-1,4-diazepan-1-yl)-N-neopentylpyrimidin-2-amine Bis(2,2,2-trifluoroacetate) **48**.* According to the general procedure, the title compound was prepared from **35** (80 mg, 0.16 mmol) over 3 h. The reaction mixture was quenched with saturated $NaHCO_{3(aq)}$ (5 mL) and extracted with EtOAc (3 × 30 mL). The organic phases were combined, washed with brine (50 mL), and dried over $MgSO_4$. After removing the solvent under reduced pressure, the product was purified by preparative HPLC [column: Phenomenex Kinetex 5u XB-C18 250 × 21.2 mm; gradient: 0−30 min: A/B 95/5−33/67 (v/v), flow 15 mL/min, t_R = 13 min] to yield **48** as colorless hygroscopic foam (60 mg, 73%). R_f = 0.8 (DCM/1.75 M NH_3 in MeOH 80/20). RP-HPLC (220 nm): 99.1% (k = 1.84). Ratio of configurational isomers evident in NMR performed in DMSO-d_6: ca 1:1.7. ^{1}H NMR (300 MHz, MeOH-d_4): δ (ppm) 7.78 (m, 1H), 6.43 (m, 1H), 3.72 (m, 10 H), 2.96 (m, 3H), 2.32 (m, 2H), 0.99 (m, 9H). ^{1}H NMR (600 MHz, DMSO-d_6): δ (ppm) 12.78 (br, 1H), 10.24 (br, 1H), 8.47 (br, 1H), 7.94 (d, J = 7.1 Hz, 1H), 6.45 (m, 1H), 3.93 (m, 6H), 3.20 (m, 4H), 2.82 (m, 3H), 2.16 (m, 2H), 0.90 (s, 9H). ^{13}C NMR (151 MHz, DMSO-d_6, HSQC, HMBC): δ (ppm) 161.76 (quat., 1C), 161.67 (quat., 1C), 158.71 (q, J = 32.0 Hz, TFA), 153.55 (quat., 1C), 153.38 (quat., 1C), 143.29, 142.99, 116.88 (q, J = 298.5 Hz, TFA), 94.63, 94.56, 54.76, 54.74, 54.59, 54.52, 51.33, 46.52, 45.13, 43.46, 43.27, 42.73, 41.20, 32.17 (quat., 1C), 27.12 (3C), 23.20, 22.95. HRMS (ESI) m/z: $[M + H]^+$ calcd for $[C_{15}H_{28}N_5]^+$, 278.2339; found, 278.2340. $C_{15}H_{27}N_5\cdots C_4H_2F_6O_4$ (277.42 + 28.05).

*General Procedure for **49**−**51**.* The respective 2,4-diaminopyrimidine bis(hydrotrifluoroacetate) (**33**−**35**) (1 equiv), 1,3-bis(*tert*-butoxycarbonyl)-2-methyl-2-thiopseudourea (1.2 equiv), $HgCl_2$ (1.5 equiv), and TEA (10 equiv) were suspended in DCM and stirred at rt for 6 h. The suspension was filtered through a Cellite pad, and the filtrate was concentrated under reduced pressure. The crude product was purified by chromatography. After the removal of the protection group with TFA in DCM (5−7 h), the product was purified by preparative HPLC.

*(R)-1-{1-[2-(Neopentylamino)pyrimidin-4-ylpyrrolidin-3-yl}-guanidine Bis(2,2,2-trifluoroacetate) **49**.* According to the general procedure, the title compound was prepared from **33** (200 mg, 0.419 mmol), 1,3-bis(*tert*-butoxycarbonyl)-2-methyl-2-thiopseudourea (146 mg, 0.503 mmol), $HgCl_2$ (171 mg, 0.626 mmol), and TEA (600 μL, 4.33 mmol) in DCM (5 mL). The crude product was purified by chromatography [DCM/MeOH 100/0−95/5 (v/v), SiO_2 40 g] to give a pale yellow sticky oil (120 mg, 58.3%). R_f = 0.4 (DCM/MeOH 90/10). Deprotection (100 mg, 0.203 mmol) in DCM (5 mL) and TFA (2 mL), followed by preparative HPLC [column: Phenomenex Kinetex 5u XB-C18 250 × 21.2 mm; gradient: 0−30 min: A/B 85.5/14.5−28.5/71.5 (v/v), flow 15 mL/min, t_R = 11.5 min] afforded **49** as colorless hygroscopic foam (72 mg, 68.1%). R_f = 0.2 (DCM/1.75 M NH_3 in MeOH 90/10). RP-HPLC (220 nm): 99.8% (k = 2.21). Ratio of configurational isomers evident in NMR performed in DMSO-d_6: is ca 1:1.7. ^{1}H NMR (300 MHz, MeOH-d_4): δ (ppm) 7.70 (m, 1H), 6.20 (m, 1H), 4.30 (m, 1H), 4.40−3.48 (m, 4H), 3.39−3.28 (m, 2H), 2.29 (m, 2H), 0.97 (s, 9H). ^{1}H NMR (600 MHz, DMSO-d_6): δ (ppm) 12.44 (br, 1H), 8.36 (m, 2H), 7.87 (m, 1H), 7.40 (m, 4H), 6.20 (m, 1H), 4.26 (m, 1H), 3.81 (m, 1H), 3.71−3.41 (m, 3H), 3.22 (m, 2H), 2.27 (m, 1H), 1.98 (m, 1H), 0.90 (s, 9H). ^{13}C NMR (151 MHz, DMSO-d_6, HSQC, HMBC): δ (ppm) 159.60 (quat., 1C), 159.47 (quat., 1C), 159.02 (q, J = 31.8 Hz, TFA), 156.46 (quat., 1C), 153.49 (quat., 1C), 153.45 (quat., 1C), 142.43, 142.32, 116.92 (q, J = 297.8 Hz, TFA), 95.52, 95.27, 52.06, 51.94, 51.29, 51.27, 50.44, 49.65, 45.24, 45.16, 32.27 (quat., 1C), 32.23 (quat., 1C), 30.63, 29.77,

DOI: 10.1021/acs.jmedchem.9b01342
J. Med. Chem. XXXX, XXX, XXX−XXX

27.15 (3C). HRMS (ESI) m/z: $[M + H]^+$ calcd for $[C_{14}H_{26}N_7]^+$, 292.2244; found, 292.2247. $C_{14}H_{25}N_7\cdots C_4H_2F_6O_4$ (291.40 + 228.05).

4-[2-(Neopentylamino)pyrimidin-4-yl]piperazine-1-carboximidamide Bis(2,2,2-trifluoroacetate) ***50***. According to the general procedure, the title compound was prepared from **34** (200 mg, 0.419 mmol), 1,3-bis(*tert*-butoxycarbonyl)-2-methyl-2-thiopseudourea (146 mg, 0.503 mmol), $HgCl_2$ (171 mg, 0.630 mmol), and TEA (600 μL, 4.33 mmol) in DCM (5 mL). The product was purified by chromatography [DCM/MeOH 100/0−95/5 (v/v), SiO_2 25 g] to give a yellow oil (200 mg, 97%). R_f = 0.3 (DCM/MeOH 95/5). Deprotection (180 mg, 0.366 mmol) in DCM (3 mL) and TFA (1 mL), followed by preparative HPLC [column: Phenomenex Kinetex 5u XB-C18 250 × 21.2 mm; gradient: 0−30 min: A/B 90/10−38/62 (v/v), flow 15 mL/min, t_R = 12.5 min] afforded **50** as colorless hygroscopic foam (50 mg, 27.0%). R_f = 0.05 (DCM/MeOH 90/10). RP-HPLC (220 nm): 99.9% (k = 2.02). ^{1}H NMR (300 MHz, MeOH-d_4): δ (ppm) 7.76 (d, J = 7.6 Hz, 1H), 6.43 (d, J = 7.5 Hz, 1H), 4.23−3.32 (m, 9H), 0.98 (s, 9H). ^{1}H NMR (600 MHz, DMSO-d_6): δ (ppm) 12.47 (br, 1H), 8.31 (br, 1H), 7.92 (d, J = 6.9 Hz, 1H), 7.57 (br, 4H), 6.49 (d, J = 7.4 Hz, 1H), 3.87 (br, 4H), 3.58 (m, 4H), 3.21 (br, 2H), 0.90 (s, 9H). ^{13}C NMR (151 MHz, DMSO-d_6, HSQC, HMBC): δ (ppm) 160.97 (quat., 1C), 158.58 (q, J = 31.2 Hz, TFA), 156.22 (quat., 1C), 153.77 (quat., 1C), 143.63, 117.15 (q, J = 300.0 Hz, TFA), 94.29, 51.35, 43.86 (2C), 42.91, 42.58, 32.28 (quat., 1C), 27.13 (3C). HRMS (ESI) m/z: $[M + H]^+$ calcd for $[C_{14}H_{26}N_7]^+$, 292.2244; found, 292.2247. $C_{14}H_{25}N_7\cdots C_4H_2F_6O_4$ (291.40 + 228.05).

4-[2-(Neopentylamino)pyrimidin-4-yl]-1,4-diazepane-1-carboximidamide Bis(2,2,2-trifluoroacetate) ***51***. According to the general procedure, the title compound was prepared from **35** (250 mg, 0.509 mmol), 1,3-bis(*tert*-butoxycarbonyl)-2-methyl-2-thiopseudourea (177 mg, 0.610 mmol), $HgCl_2$ (207 mg, 0.762 mmol), and TEA (705 μL, 5.41 mmol) in DCM (5 mL). The product was purified by chromatography [DCM/MeOH 100/0−95/5 (v/v), SiO_2 35 g] to give a pale yellow sticky foam (240 mg, 94%). R_f = 0.3 (DCM/MeOH 95/5). Deprotection (230 mg, 0.37 mmol) in DCM (5 mL) and TFA (1 mL), followed by preparative HPLC [column: Phenomenex Kinetex 5u XB-C18 250 × 21.2 mm; gradient: 0−30 min: A/B 90/10−48/52 (v/v), flow 20 mL/min, t_R = 12 min] afforded **51** as colorless hygroscopic foam (90 mg, 37.1%). R_f = 0.05 (DCM/MeOH 95/5). RP-HPLC (220 nm): 99.8% (k = 2.09). Ratio of configurational isomers evident in NMR performed in DMSO-d_6: ca 1:1.4. ^{1}H NMR (300 MHz, MeOH-d_4): δ (ppm) 7.75 (d, J = 7.5 Hz, 1H), 6.43 (m, 1H), 4.15 (m, 1.2H), 3.97 (m, 1.5 H), 3.79 (m, 3H), 3.64 (m, 2H), 1.98 (m, 2H), 0.98 (m, 9H). ^{1}H NMR (600 MHz, DMSO-d_6): δ (ppm) 12.74 (br, 1H), 8.41 (br, 1H), 7.91 (m, 1H), 7.51 (br, 4H), 6.45 (d, J = 7.4 Hz, 1H), 3.59 (m, 10H), 1.83 (m, 2H), 0.90 (s, 9H). ^{13}C NMR (151 MHz, DMSO-d_6, HSQC, HMBC): δ (ppm) 161.25 (quat., 1C), 158.86 (q, J = 31.5 Hz, TFA), 155.93 (quat., 1C), 153.84 (quat., 1C), 153.76 (quat., 1C), 143.60, 117.07 (d, J = 297.8 Hz, TFA), 94.15, 51.39, 47.42, 47.30, 46.86, 46.73, 46.72, 46.67, 46.34, 46.02, 32.15 (quat., 1C), 27.13 (3C), 25.17, 24.08. HRMS (ESI) m/z: $[M + H]^+$ calcd for $[C_{15}H_{28}N_7]^+$, 306.2401; found, 306.2402. $C_{15}H_{27}N_7\cdots C_4H_2F_6O_4$ (305.43 + 228.05).

(R)-N-{1-[2-(Neopentylamino)pyrimidin-4-yl]pyrrolidin-3-yl}propionamide 2,2,2-Trifluoroacetate ***52***. **33** (100 mg, 0.209 mmol), DIPEA (630 μL, 3.70 mmol), and 1-propionylpyrrolidine-2,5-dione (70 mg, 0.41 mmol) were dissolved in DCM (5 mL). The reaction was stirred at rt for 24 h. The solvent was removed under reduced pressure, and the crude product was purified by preparative HPLC [column: Phenomenex Kinetex 5u XB-C18 250 × 21.2 mm; gradient: 0−30 min: A/B 80.7/19.3−88/62 (v/v), flow 20 mL/min, t_R = 11 min] to yield **52** as colorless hygroscopic powder (50 mg, 56.9%). RP-HPLC (220 nm): 97.9% (k = 3.34). Ratio of configurational isomers evident in NMR: ca 1:1.4. ^{1}H NMR (600 MHz, DMSO-d_6): δ (ppm) 12.30 (br, 1H), 8.24 (br, 1H), 8.10 (m, 1H), 7.83 (m, 1H), 6.17 (m, 1H), 4.36 (m, 1H), 3.67 (m, 3H), 3.46 (m, 0.5H), 3.32 (m, 0.5H); 3.21 (m, 2H), 2.07 (m, 3H), 1.89 (m, 1H), 0.98 (m, 3H), 0.90 (m, 9H). ^{13}C NMR (151 MHz, DMSO-d_6, HSQC, HMBC): δ (ppm) 172.92 (quat., 1C), 159.36 (quat., 1C), 159.27 (quat., 1C), 158.63 (q, J = 32.0 Hz, TFA), 153.40 (quat., 1C), 142.07, 116.90 (q, J = 298.7 Hz, TFA), 95.51, 95.34, 52.32, 52.22, 51.25, 48.40, 47.55, 45.47, 45.41, 32.22 (quat., 1C), 30.48, 29.61, 28.26, 27.15 (3C), 9.73. HRMS (ESI) m/z: $[M + H]^+$, calcd for $[C_{16}H_{28}N_5O]^+$, 306.2288; found, 306.2291. $C_{16}H_{27}N_5\cdots C_2HF_3O_2$ (305.43 + 114.02).

Chemical Stability. The chemical stability of **43**, **46**, **48**, and **49** was investigated in PBS (pH 7.4) at 23 °C over 24 h. For this purpose, 200 μM dilutions in PBS (stock solution: 10 mM in DMSO) were prepared and incubated. After 0, 1, 5, and 24 h, 100 μL of this solution was added to 100 μL of MeCN/0.5% TFA 10/90 (v/v). This solution was filtered through PTFE filters prior to analysis by RP-HPLC (conditions for analytical HPLC see General Experimental Conditions, Graphs see Figures S33−S36 in the Supporting Information). Injection volume: 70 μL; k = 2.02 (**43**), k = 1.95 (**46**), k = 1.89 (**48**), k = 2.26 (**49**).

Synthesis of Radioligand [^{3}H]46. Compound [^{3}H]**46** was essentially prepared according to a previously described radiolabeling protocol,[46] using succinimidyl [^{3}H]propionate as tritiated precursor, with the following modifications:

The amine precursor **45** was methylated with commercially available methyl nosylate [methyl-^{3}H] ([^{3}H]**53**), dissolved in MeCN (specific activity 60−80 Ci/mmol, 2.22−2.96 TBq/mmol, activity concentration 100 mCi/mL, Biotrend Chemikalien GmbH, Köln, Germany). Therefore, in a 2 mL reaction vessel with a screw cap, 11.5 μL of a solution of **45** in acetone (67.8 mM, 0.775 μmol, 6.2 equiv) and pestled K_2CO_3 (6.378 μmol, 51 equiv) were suspended in MeCN (124.3 μL) and transferred into a glass ampule containing 100 μL of [^{3}H]**53** in MeCN (0.125 μmol, 1 equiv, 10 mCi). The 2 mL reaction vessel was washed with 124.3 μL of MeCN, and the same volume was transferred to the reaction mixture, too. The reaction mixture was stirred at room temperature for 22.5 h, before the reaction was quenched with 40 μL of $TFA_{(aq)}$ (10%). The solvent was removed in a vacuum concentrator within 45 min. The residual material was diluted to a final volume of 800 μL with a mixture of MeOH/0.05% TFA 8/92 (v/v) for the purification, using an analytical HPLC system (Waters, Eschborn, Germany) consisting of two 510 pumps, a pump control module, a 486 UV/vis detector, and a Flow-one Beta series A-500 radio detector (Packard, Meriden, CT). As the stationary phase, a Luna C18 (3 μm, 150 mm × 4.6 mm, Phenomenex, Aschaffenburg, Germany) column was used at a flow rate of 0.7 mL/min. The mobile phase consisted of MeOH + 0.05% TFA (A) and 0.05% TFA (B). Isolation of [^{3}H]**46** was performed by performing 10 HPLC runs with injection volumes of 80 μL (only UV detection at 220 nm), applying the following conditions: 0−26 min, A/B 18.5/81.5; 26−27 min, 18.5/81.5−95/5; 27−34 min, 95/5; $t_R \approx$ 25 min. The fractions containing the radioligand were collected in 2 mL reaction vessels with screw caps and the volumes were reduced in a vacuum concentrator to a final volume of 163.3 μL. After EtOH (381 μL) was added, the solution was transferred to a 3-mL borosilicate glass vial with conical bottom (Wheaton, NextGen 3 mL V-vials). The reaction vessels were washed twice with EtOH/H_2O 70/30 (v/v), and the volumes were combined to obtain the tentative stock solution (846 μL). For quantification, a four-point calibration curve with unlabeled **46** [0.5, 1, 2, 5 μM in MeCN/0.05% TFA 8/92 (v/v)] was constructed. For this purpose, the above described HPLC system was used under the following modified conditions: 0−16 min, MeCN + 0.04% TFA/0.05% TFA 12/88; 16−19 min, 12/88−95/5; 19−26 min, 95/5; injection volume: 100 μL; flow rate 1 mL/min; UV detection at 220 nm; t_R = 15.0 min. An aliquot of the tentative stock (2 μL) was diluted with MeCN/0.05% TFA 8/92 (v/v) (128 μL), and 100 μL of this solution was analyzed by HPLC, 2 μL was added to 3 mL of Rotiszint eco plus (Carl Roth, Karlsruhe, Germany), and five replicates were counted with a LS 6500 liquid scintillation counter (Beckmann Coulter, München, Germany). This procedure was repeated. The molarity of the tentative stock was calculated from the mean of the peak areas and determined calibration curve. A solution of [^{3}H]**46** [final concentration: 1 μM in MeCN/0.05% TFA (8/92 v/v)] was spiked with unlabeled **46** [final concentration: 1 mM, in MeCN/0.05% TFA (8/92 v/v)] and analyzed by HPLC (0−15 min, MeCN +0.04% TFA/0.05% TFA 10/90−32.5/67.5; 15−25 min, 32.5/67.5−90/10; 25−35 min, 90/10; flow rate 0.8 mL/min;

DOI: 10.1021/acs.jmedchem.9b01342
J. Med. Chem. XXXX, XXX, XXX−XXX

injection volume 100 μL; UV detection at 220 nm) and radiometric detection (flow rate of the liquid scintillator [Rotiszint eco plus/MeCN (85/15 v/v): 4 mL/min] to confirm the chemical identity (t_R = 11.1 min) and to determine the radiochemical purity (99%). After storage at −20 °C for 11 months, this experiment was repeated, giving a radiochemical purity of 94%. Calculated specific activity: 1.59 TBq/mmol (43.08 Ci/mmol). The final activity concentration was adjusted to 58.1 MBq/mL (1.6 mCi/mL) by adding EtOH/H_2O (70/30 v/v) to come to a molarity of 36.4 μM. Radiochemical yield: 108.54 MBq, 29%.

Cell Culture, Transfection, and Preparation of Cell Membranes and Homogenates. General procedures for the generation of recombinant baculoviruses, culture of *Sf*9 cells, and membrane preparation were described previously.[16,53] The generation and culture of HEK293T-SF-hH_4R-His6-CRE-Luc, HEK293T-SF-mH_4R-His6-CRE-Luc, and HEK293T-SF-rH_4R-His6-CRE-Luc cells were described previously.[26] In contrast to the published procedure, HEK293T-SF-mH_4R-His6-CRE-Luc cells were cultured in the presence of 700 μg/mL of hygromycin B (A.G. Scientific, San Diego, USA). Cell homogenates were prepared after growing the cells in 30 culture dishes (145 cm^2) to 80% confluency in a humidified atmosphere (95% air, 5% CO_2, 37 °C), using Dulbecco's modified Eagle medium (DMEM) (Sigma-Aldrich, Deisenhofen, Germany) and 10% fetal calf serum (FCS) (Biochrom, Berlin, Germany). Subsequently, the cells were rinsed with PBS (10 mL/dish, 100 mM NaCl, 80 mM Na_2HPO_4, 20 mM NaH_2PO_4, pH 7.4) and scraped off the dish using a sterile cell scraper in the presence of a harvest buffer[54] [7 mL/dish, 10 mM Tris-HCl, 0.5 mM ethylenediaminetetraacetic acid (EDTA), 5.5 mM KCl, 140 mM NaCl, pH 7.4]. After centrifugation (1000 rpm, 10 min), the cells were suspended in ice-cold homogenate buffer[54] (15 mL, 50 mM Tris−HCl, 5 mM EDTA, 1.5 mM $CaCl_2$, 5 mM $MgCl_2$, 120 mM NaCl, pH 7.4) and supplemented with protease inhibitors (SigmaFAST, Cocktail Tablets, EDTA-free, Sigma-Aldrich, Deisenhofen, Germany). Afterward, the cells were lysed (20 000 rpm/min, 5 × 5 s, ice-cooled, Ultra-TURRAX, Janke & Kunkel, IKA-Werke GmbH & Co. KG, Staufen, Germany), and the lysate was centrifuged (23 000 rpm, 45 min, 4 °C, Optima-L70-Preparative Ultracentrifuge, Beckmann Coulter, München, Germany). The remaining pellets were suspended in ice-cold binding buffer[53] (15 mL, 12.5 mM $MgCl_2$, 1 mM EDTA, 75 mM Tris-HCl, pH 7.4), homogenized with a Dounce homogenizer (10 times, ice-cooled), and stored at −80 °C in small aliquots (0.2 mL, 0.5 mL).

HEK293T cells, stably expressing xH_4R-ELucC/ELucN-β-arrestin2 (x = h, m, r), were generated as follows: the cDNAs, encoding the C-terminal luciferase fragment of the emerald luciferase (ELucC)[55] fused to the C-terminus of either hH_4R, mH_4R, or rH_4R, were generated by replacing the hH_1R in the previously described pcDNA4 hH_1R-ELucC vector[56] by each xH_4R cDNA without their stop codons. Then, HEK293T cells stably expressing the ELucN-β-arrestin2 construct[56] were stably transfected with each pcDNA4 xH_4R-ELucC vector as described.[56] The HEK293T-β-arr2-hH_4R, HEK293T-β-arr2-mH_4R, and HEK293T-β-arr2-rH_4R cells were cultivated as previously described for HEK293T-β-arr2-hH_1R cells.[56]

Radioligand Binding Experiments. Competition binding experiments on membrane preparations of *Sf*9 insect cells, expressing the hH_1R + RGS4, hH_2R-$Gs_{\alpha s}$, hH_3R + $Gi_{\alpha 2}$ + $\beta_1\gamma_2$, or hH_4R + $Gi_{\alpha 2}$ + $\beta_1\gamma_2$, were essentially performed as described previously[57] with the following modifications: the experiments were performed in 96-well plates (PP microplates 96 well, Greiner Bio-One, Frickenhausen, Germany) in a total volume of 100 μL, containing 5−25 μg (hH_4R), 24−35 μg (hH_3R), 15 μg (hH_2R), and 23 μg (hH_1R) of soluble membrane protein and 0.2% BSA (bovine serum albumin). Used radioligands: hH_1R: [^{3}H]pyrilamine (c = 5 nM, specific activity 85.3 Ci/mmol, K_d = 4.5 nM,[57] Hartmann Analytics GmbH, Braunschweig, Germany), hH_2R: [^{3}H]UR-DE257[28] (c = 30 nM, specific activity 63.0 Ci/mmol, K_d = 31 ± 5 nM), hH_3R: [^{3}H]UR-PI294[12] ([^{3}H]**2**) (c = 2 nM, specific activity 93.3 Ci/mmol, K_d = 1.1 ± 0.2 nM) or [^{3}H]N^α-methylhistamine (c = 3 nM, specific activity 85.3 Ci/mmol, K_d = 3 nM,[57] Hartmann Analytics GmbH, Braunschweig, Germany) and hH_4R: [^{3}H]histamine ([^{3}H]**1**) (c = 10 or 40 nM depending on the used batches, specific activity 25.0 Ci/mmol, K_d = 15 nM or 47.5 nM depending on the batches, Biotrend Chemikalien GmbH, Köln, Germany) or [^{3}H]UR-PI294[12] (c = 5 nM, specific activity 93.3 Ci/mmol, K_d = 5.1 ± 1.9 nM).

For competition binding, saturation binding and kinetic binding experiments with [^{3}H]**46**, the radioligand solution [36.4 μM in EtOH/H_2O 70/30 (v/v)] was mixed with a solution of "cold" **46** ([6.4 μM in EtOH/H_2O 70/30 (v/v)] (1/3) because of economic reasons. The HEK293T-SF-hH_4R-His6-CRE-Luc-, HEK293T-SF-mH_4R-His6-CRE-Luc-, or HEK293T-SF-rH_4R-His6-CRE-Luc cell homogenates were thawed and sedimented by centrifugation (16 100 g, 4 °C, 10 min) before the supernatant was discarded. The pellets were suspended in ice-cooled binding buffer to come to 1.8 μg (hH_4R), 2.8 μg (mH_4R), and 3.1 μg (rH_4R) protein per μL of binding buffer. The experiments were performed in 96-well plates (PP microplates 96 well, Greiner Bio-One, Frickenhausen, Germany) in a total volume of 100 μL containing 18 μg (hH_4R), 28 μg (mH_4R), and 31 μg (rH_4R) homogenate protein and 0.2% BSA. After different incubation periods at room temperature, the previously described procedure[57] for competition binding experiments using *Sf*9 cell membranes was followed.

In competition binding experiments, the concentration of [^{3}H]**46** was 40 nM (hH_4R) 30 nM (rH_4R), or 20 nM (mH_4R), while increasing concentrations of unlabeled ligands (**1**, **4**, **5**, and **6**) were applied. The plates were shaken at 250 rpm for 60 min. For the analysis of the data obtained from experiments on *Sf*9 membranes, total binding (dpm) was plotted versus log (concentration competitor) and normalized [1.0 = bound radioligand (dpm) in the absence of competitor, 0.0 = non-specifically bound radioligand (dpm) in the presence of **1** (10 μM, h$H_{3,4}$R), diphenhydramine (10 μM, hH_1R), or famotidine (100 μM, hH_2R)]. For competition binding experiments at HEK293T-CRE-Luc cell homogenates, total binding (dpm) was plotted versus log (concentration competitor) and normalized [1.0 = bound radioligand (dpm) in the absence of a competitor, 0.0 = nonspecifically bound radioligand (dpm) in the presence of **6** (100 μM, h, m, r H_4R)]. Applying a four-parameter logistic equation (log-(inhibitor) versus response−variable slope) (GraphPad Prism Software 7.1, San Diego, CA), pIC_{50} values and IC_{50} values were obtained for each individual experiment. The pIC_{50} values were converted to pK_i values and the IC_{50} values to K_i values by applying the Cheng−Prusoff equation[58] followed by calcuation of mean pK_i (Table 1, Table 4) and mean K_i (for the calculation of $H_{2\text{-}4}$R subtype selectivity, Table 1).

Saturation binding experiments were conducted with various concentrations of [^{3}H]**46**, while nonspecific binding was determined in the presence of **6** (1000-fold excess to each [^{3}H]**46** concentration). The plates were shaken at 250 rpm for 60 min. Specific binding data (dpm) were plotted against the free radioligand concentration (nM) and analyzed by a two-parameter equation describing hyperbolic binding to obtain K_d and B_{max} values (GraphPad Prism 7.1). The free radioligand concentration is the difference between the amount of specifically bound radioligand (nM) (calculation includes the amount of specifically bound [^{3}H]**46** in dpm, the specific activity of [^{3}H]**46** and the volume per well) and total radioligand concentration. Nonspecific binding data were fitted by linear regression (GraphPad Prism 7.1).

For association experiments, the h, m, or rH_4R expressing homogenates were incubated with [^{3}H]**46** (40 nM hH_4R, 30 nM rH_4R, 20 nM mH_4R). Incubation was stopped after different time points (0−45 min) by addition of **6** (1000-fold excess to the [^{3}H]**46** concentration). Nonspecific binding was determined in the presence of **6** (1000-fold excess to the [^{3}H]**46** concentration). The plates were shaken at 250 rpm throughout. In dissociation experiments, the h, m, or rH_4R expressing homogenates were incubated with [^{3}H]**46** (40 nM hH_4R, 30 nM rH_4R, 20 nM mH_4R) for 30 min, before **6** (1000-fold excess to the [^{3}H]**46** concentration) was added at different time points (0−90 min). For the determination of the nonspecific binding, the procedure was performed identically, but **6** (1000-fold excess to the [^{3}H]**46** concentration) was added during the incubation step. The

DOI: 10.1021/acs.jmedchem.9b01342
J. Med. Chem. XXXX, XXX, XXX−XXX

plates were shaken at 250 rpm throughout. The specific binding data (dpm) from association experiments were analyzed by a two-parameter equation describing exponential incline (GraphPad Prism 7.1) to a maximum to obtain k_{obs} (observed association rate constant) and $B_{(eq)}$ (maximum of specifically bound radioligand), used for the calculation of specifically bound radioligand ($B_{(t)}$) in %, which is plotted over time. In dissociation experiments, $B_{(t)}$ (%) were plotted over time and analyzed by a three-parameter equation describing exponential decline (GraphPad Prism 7.1) to obtain the dissociation rate constant k_{off} and $B_{(plateau)}$ (%, bottom of specifically bound radioligand).

Luciferase Reporter Gene Assay. The luciferase reporter gene assay, using HEK293T-SF-hH_4R-His6-CRE-Luc, HEK293T-SF-mH_4R-His6-CRE-Luc, or HEK293T-SF-rH_4R-His6-CRE-Luc cells, was performed as described previously,[26] applying the following modifications:

After seeding 0.8×10^5 (hH_4R) and 1.6×10^5 (r,mH_4R) cells per well (160 μL) into colorless flat-bottomed 96-well plates (Greiner, Frickenhausen, Germany), they were allowed to attach for 17−24 h in a humidified atmosphere (95% air, 5% CO_2, 37 °C), using DMEM without phenol red supplemented with 5% (v/v) FCS. A stock solution (10 mM) of forskolin (Sigma-Aldrich) in DMSO was used to prepare the feed solution in DMEM without phenol red [5% (v/v) FCS]. Forskolin solution (20 μL, final concentration: 0.5 μM for hH_4R, 1.0 μM for m and rH_4R) and 20 μL of a 10-fold concentrated solution of the respective compound in various concentrations [10 mM stock solutions (see General Experimental Conditions) diluted with DMEM] was added. The cells were incubated for 5 h in a humidified atmosphere (95% air, 5% CO_2, 37 °C). The final DMSO concentration in the assay did not exceed 1%. Afterwards, all media were discarded, followed by the addition of 80 μL of lysis buffer[26] to each well. The cells were shaken at room temperature for 30−45 min(180 rpm). For the luminescence measurement, 40 μL of the lysate was transferred to a white flat-bottomed 96-well plate (Greiner) and was supplemented with 80 μL of luciferase assay buffer[26] (120 μL/well). Luminescence, expressed as RLUs (relative light units), was measured for 1 s per well using the GENios Pro microplate reader (Tecan, Salzburg, Austria) or the EnSpire multimode reader (PerkinElmer, Waltham, USA). Data were processed by plotting the RLUs versus log (concentration agonist) followed by a normalization (1.0 = forskolin-stimulated luciferase activity, 0.0 = induced change in forskolin-stimulated luciferase activity caused by 10 μM of the endogenous agonist histamine **1**) and transformation step (standard function in GraphPad Prism 7.1: $Y = 1.0 - Y$). The analysis of the data was performed applying a four-parameter logistic equation (log(agonist) vs response−variable slope, GraphPad Prism 7.1).

β-Arrestin2 Recruitment Assay. The recruitment of the β-arrestin2 was measured via split-luciferase complementation. Agonist potencies were determined using HEK293T cells, stably expressing xH_4R-ELucC/ELucN-β-arrestin2 (x = h, m, r), using the GENios Pro microplate reader (Tecan, Salzburg, Austria) as previously described for HEK293T-β-arr1-H_1R and HEK293T-β-arr2-H_1R cells.[56] Data were processed by plotting the RLUs versus log (concentration agonist) followed by a normalization step (agonist mode: 1.0 = maximum of β-arrestin2 recruitment caused by 100 μM of the endogenous agonist histamine **1**, 0.0 = basal activity). The normalized data were analyzed by applying a four-parameter logistic equation (log(agonist) versus response−variable slope) (GraphPad Prism 7.1). In antagonist mode, the solutions containing the antagonist were pre-incubated for 15 min before a histamine **1** solution in H_2O (final concentrations in assay: 10 μM) was added. Data from antagonist mode were processed by plotting the RLUs versus log (concentration antagonist) followed by a normalization step (1.0 = β-arrestin2 recruitment caused by 10 μM of the endogenous agonist **1**, 0.0 = basal activity).

Screening for Activity at mH_4R and rH_4R in β-Arrestin Recruitment- and Luciferase Reporter Gene Assays. Data of agonist mode and antagonist mode (performed if $\alpha < 0.1$) were processed and normalized as described above for the respective functional assay and were plotted as bar graphs (GraphPad Prism Software 7.1). The pEC_{50}/pIC_{50} values and efficacies (α) were estimated based on the screening of three distinct concentrations (final: 100 nM, 1 μM, 10 μM) for each investigated compound. (Results see Table S1 in the Supporting Information).

■ ASSOCIATED CONTENT

Supporting Information

The Supporting Information is available free of charge on the ACS Publications website at DOI: 10.1021/acs.jmedchem.9b01342.

Preparation and source of the intermediate compounds **7**−**18** and **20**−**31**; screening for activity of **34**, **36**, **37**, **39**−**42**, **44**, **47**, and **50**−**52** in the luciferase reporter gene- and the β-arrestin2 recruitment assays at the mouse and rat H_4R; bias analysis for compounds **33**, **35**, **38**, **43**, **45**, **46**, **48**, and **49**; ^{1}H NMR and ^{13}C NMR spectra of the target compounds **33**, **35**, **38**, **41**, **43**, **44**−**46**, **48**, and **49**; RP-HPLC chromatograms of compounds **33**−**52**; RP-HPLC chromatograms: chemical stability of **43**, **46**, **48**, and **49** (PDF)

Molecular formula strings, hH_{1-4}R binding data, and h/m/rH_4Rs functional data and thermodynamically and kinetically derived binding constants of [^{3}H]**46** for the h/m/rH_4Rs (CSV)

■ AUTHOR INFORMATION

Corresponding Authors

*E-mail: edith.bartole@ur.de. Phone: (+49)941-943-2925. Fax: (+49)941-943-4820 (E.B.).

*E-mail: guenther.bernhardt@ur.de. Phone: (+49)941-943-4822. Fax: (+49)941-943-4820 (G.B.).

ORCID

Edith Bartole: 0000-0001-5387-7920

Takeaki Ozawa: 0000-0002-3198-4853

Armin Buschauer: 0000-0002-9709-1433

Günther Bernhardt: 0000-0001-6491-9874

Present Address

[§]AbbVie Deutschland GmbH & Co. KG, 67061 Ludwigshafen am Rhein, Germany.

Author Contributions

E.B. conceived the project with input from A.B and G.B. E.B. synthesized compounds, performed experiments, and data analysis with supervision from A.B. and G.B. M.T. cloned the vector hH_4R-ELucC/ELucN-β-arrestin2 under supervision of T.O. T.L. cloned the vectors mH_4R-ELucC/ELucN-β-arrestin2 and rH_4R-ELucC/ELucN-β-arrestin2 under supervision of G.B. and A.B. E.B. and G.B. wrote the manuscript with input from all co-authors.

Funding

This work was funded by the Graduate Training Program GRK1910 of the Deutsche Forschungsgesellschaft (DFG) (E.B., T.L., G.B. and A.B.) and the Elite Network of Bavaria (T.L. and A.B.).

Notes

The authors declare no competing financial interest.

[‖]Deceased, July 18, 2017.

■ ACKNOWLEDGMENTS

The authors thank: Dr. Max Keller for his insightful advice on radiosynthesis and miscellaneous matters and Maria Beer-Krön, Susanne Bollwein and Dita Fritsch for excellent technical

DOI: 10.1021/acs.jmedchem.9b01342
J. Med. Chem. XXXX, XXX, XXX−XXX

assistance. We also thank Dr. Patrick Igel for providing compounds **17** and **18** and Dr. Paul Baumeister for providing 1,3-bis(*tert*-butoxycarbonyl)-2-methyl-2-thiopseudourea.

■ ABBREVIATIONS

α, instrinsic activity; AU, absorption units; Bq, becquerel; $CDCl_3$, deuterated chloroform; cpm, counts per minute; DIPEA, diisopropylethylamine;; DMEM, Dulbecco's modified Eagle medium; dpm, desintegrations per minute; EtOAc, ethyl acetate; EtOH, ethanol; GTPase, hydrolase enzyme that can bind and hydrolyse guanosine triphosphate (GTP); GTPγS, guanosine 5′-thiotriphosphate; H_{1-4}Rs, the histamine receptor family; HEK293T, human embryonic kidney 293T cells; *i*-PrOH, isopropyl alcohol; K_b, dissociation constant obtained from functional assays; K_d, dissociation (or binding) constant obtained from a saturation binding experiment; K_i, dissociation (or binding) constant obtained from a competition binding experiment; MeCN, acetonitrile; MeOH, methanol; ON, overnight; Pd/C, palladium on activated charcoal; PE, petroleum ether; pEC_{50}, negative logarithm of the half-maximum activity concentration in M; pIC_{50}, negative logarithm of the half-maximum inhibitory concentration in M; pK_b, negative logarithm of the K_b in M; pK_i, negative logarithm of the K_i in M; ppm, parts per million; RP-HPLC, reversed-phase HPLC; rt, room temperature; SEM, standard error of the mean; *Sf*9, Spodoptera frugiperda insect cell line; TEA, triethylamine; Tris-HCl, tris(hydroxymethyl)-aminomethane hydrochloride; Trt, trityl, triphenylmethyl protecting group; $\Delta\Delta\log(\tau/K_A)$, bias factor; [RL], concentration of radioligand

■ REFERENCES

(1) Nakamura, T.; Itadani, H.; Hidaka, Y.; Ohta, M.; Tanaka, K. Molecular cloning and characterization of a new human histamine receptor, hH4R. *Biochem. Biophys. Res. Commun.* **2000**, *279*, 615−620.

(2) Oda, T.; Morikawa, N.; Saito, Y.; Masuho, Y.; Matsumoto, S.-i. Molecular cloning and characterization of a novel type of histamine receptor preferentially expressed in leukocytes. *J. Biol. Chem.* **2000**, *275*, 36781−36786.

(3) Liu, C.; Ma, X.-J.; Jiang, X.; Wilson, S. J.; Hofstra, C. L.; Blevitt, J.; Pyati, J.; Li, X.; Chai, W.; Carruthers, N.; Lovenberg, T. W. Cloning and Pharmacological Characterization of a Fourth Histamine Receptor (H_4) Expressed in Bone Marrow. *Mol. Pharmacol.* **2001**, *59*, 420−426.

(4) Morse, K. L.; Behan, J.; Laz, T. M.; West, R. E.; Greenfeder, S. A.; Anthes, J. C.; Umland, S.; Wan, Y. T.; Hipkin, R. W.; Gonsiorek, W.; Shin, N.; Gustafson, E. L.; Qiao, X. D.; Wang, S. K.; Hedrick, J. A.; Greene, J.; Bayne, M.; Monsma, F. J. Cloning and characterization of a novel human histamine receptor. *J. Pharmacol. Exp. Ther.* **2001**, *296*, 1058−1066.

(5) Zhu, Y.; Michalovich, D.; Wu, H.-L.; Tan, K. B.; Dytko, G. M.; Mannan, I. J.; Boyce, R.; Alston, J.; Tierney, L. A.; Li, X.; Herrity, N. C.; Vawter, L.; Sarau, H. M.; Ames, R. S.; Davenport, C. M.; Hieble, J. P.; Wilson, S.; Bergsma, D. J.; Fitzgerald, L. R. Cloning, expression, and pharmacological characterization of a novel human histamine receptor. *Mol. Pharmacol.* **2001**, *59*, 434−441.

(6) Nguyen, D. N.; Stump, C. A.; Walsh, E. S.; Fernandes, C.; Davide, J. P.; Ellis-Hutchings, M.; Robinson, R. G.; Williams, T. M.; Lobell, R. B.; Huber, H. E.; Buser, C. A. Potent inhibitors of farnesyltransferase and geranylgeranyltransferase-I. *Bioorg. Med. Chem. Lett.* **2002**, *12*, 1269−1273.

(7) O'Reilly, M.; Alpert, R.; Jenkinson, S.; Gladue, R. P.; Foo, S.; Trim, S.; Peter, B.; Trevethick, M.; Fidock, M. Identification of a Histamine H_4 Receptor on Human Eosinophils-role in Eosinophil Chemotaxis. *J. Recept. Signal Transduction Res.* **2002**, *22*, 431−448.

(8) Thurmond, R. L.; Venable, J.; Savall, B.; La, D.; Snook, S.; Dunford, P. J.; Edwards, J. P. Clinical Development of Histamine H_4 Receptor Antagonists. *Histamine and Histamine Receptors in Health and Disease*; Handbook of Experimental Pharmacology; Springer, 2017, Vol. *241*, pp 301−320.

(9) Neumann, D. Role of the Histamine H_4-Receptor in Bronchial Asthma. *Histamine and Histamine Receptors in Health and Disease*; Handbook of Experimental Pharmacology; Springer, 2017, Vol. *241*, pp 347−359.

(10) Schneider, E. H.; Seifert, R. The histamine H_4-receptor and the central and peripheral nervous system: A critical analysis of the literature. *Neuropharmacology* **2016**, *106*, 116−128.

(11) Tichenor, M. S.; Thurmond, R. L.; Venable, J. D.; Savall, B. M. Functional Profiling of 2-Aminopyrimidine Histamine H_4 Receptor Modulators. *J. Med. Chem.* **2015**, *58*, 7119−7127.

(12) Igel, P.; Schnell, D.; Bernhardt, G.; Seifert, R.; Buschauer, A. Tritium-Labeled N^1-[3-(1H-imidazol-4-yl)propyl]-N^2-propionylguanidine ([^{3}H]UR-PI294), a High-Affinity Histamine H^3 and H^4 Receptor Radioligand. *ChemMedChem* **2009**, *4*, 225−231.

(13) Lim, H. D.; Adami, M.; Guaita, E.; Werfel, T.; Smits, R. A.; de Esch, I. J.; Bakker, R. A.; Gutzmer, R.; Coruzzi, G.; Leurs, R. Pharmacological characterization of the new histamine H_4 receptor agonist VUF 8430. *Br. J. Pharmacol.* **2009**, *157*, 34−43.

(14) Lim, H. D.; van Rijn, R. M.; Ling, P.; Bakker, R. A.; Thurmond, R. L.; Leurs, R. Evaluation of histamine H_1-, H_2-, and H_3-receptor ligands at the human histamine H_4 receptor: identification of 4-methylhistamine as the first potent and selective H_4 receptor agonist. *J. Pharmacol. Exp. Ther.* **2005**, *314*, 1310−1321.

(15) Jablonowski, J. A.; Grice, C. A.; Chai, W.; Dvorak, C. A.; Venable, J. D.; Kwok, A. K.; Ly, K. S.; Wei, J.; Baker, S. M.; Desai, P. J.; Jiang, W.; Wilson, S. J.; Thurmond, R. L.; Karlsson, L.; Edwards, J. P.; Lovenberg, T. W.; Carruthers, N. I. The First Potent and Selective Non-Imidazole Human Histamine H_4 Receptor Antagonists. *J. Med. Chem.* **2003**, *46*, 3957−3960.

(16) Schnell, D.; Brunskole, I.; Ladova, K.; Schneider, E. H.; Igel, P.; Dove, S.; Buschauer, A.; Seifert, R. Expression and functional properties of canine, rat, and murine histamine H_4 receptors in Sf9 insect cells. *Naunyn-Schmiedeberg's Arch. Pharmacol.* **2011**, *383*, 457−470.

(17) Wifling, D.; Löffel, K.; Nordemann, U.; Strasser, A.; Bernhardt, G.; Dove, S.; Seifert, R.; Buschauer, A. Molecular determinants for the high constitutive activity of the human histamine H_4 receptor: functional studies on orthologues and mutants. *Br. J. Pharmacol.* **2015**, *172*, 785−798.

(18) Seifert, R.; Strasser, A.; Schneider, E. H.; Neumann, D.; Dove, S.; Buschauer, A. Molecular and cellular analysis of human histamine receptor subtypes. *Trends Pharmacol. Sci.* **2013**, *34*, 33−58.

(19) Schneider, E. H.; Schnell, D.; Papa, D.; Seifert, R. High constitutive activity and a G-protein-independent high-affinity state of the human histamine H_4-receptor. *Biochemistry* **2009**, *48*, 1424−1438.

(20) Wifling, D.; Bernhardt, G.; Dove, S.; Buschauer, A. The extracellular loop 2 (ECL2) of the human histamine H_4 receptor substantially contributes to ligand binding and constitutive activity. *PLoS One* **2015**, *10*, No. e0117185.

(21) Liu, C.; Wilson, S. J.; Kuei, C.; Lovenberg, T. W. Comparison of human, mouse, rat, and guinea pig histamine H_4 receptors reveals substantial pharmacological species variation. *J. Pharmacol. Exp. Ther.* **2001**, *299*, 121−130.

(22) Lim, H. D.; de Graaf, C.; Jiang, W.; Sadek, P.; McGovern, P. M.; Istyastono, E. P.; Bakker, R. A.; de Esch, I. J. P.; Thurmond, R. L.; Leurs, R. Molecular determinants of ligand binding to H_4R species variants. *Mol. Pharmacol.* **2010**, *77*, 734−743.

(23) Thurmond, R. L.; Desai, P. J.; Dunford, P. J.; Fung-Leung, W.-P.; Hofstra, C. L.; Jiang, W.; Nguyen, S.; Riley, J. P.; Sun, S.; Williams, K. N.; Edwards, J. P.; Karlsson, L. A potent and selective histamine H_4 receptor antagonist with anti-inflammatory properties. *J. Pharmacol. Exp. Ther.* **2004**, *309*, 404−413.

(24) Lim, H. D.; Jongejan, A.; Bakker, R. A.; Haaksma, E.; de Esch, I. J. P.; Leurs, R. Phenylalanine 169 in the second extracellular loop of

DOI: 10.1021/acs.jmedchem.9b01342
J. Med. Chem. XXXX, XXX, XXX−XXX

the human histamine H_4 receptor is responsible for the difference in agonist binding between human and mouse H_4 receptors. *J. Pharmacol. Exp. Ther.* **2008**, *327*, 88−96.
(25) Baumeister, P. Molecular Tools for G-Protein Coupled Receptors: Synthesis, Pharmacological Characterization and [^{3}H]-Labeling of Subtype-Selective Ligands for Histamine H_4 and NPY Y_2 Receptors. Ph.D Dissertation, University of Regensburg, 2014. http://epub.uni-regensburg.de/30505.
(26) Nordemann, U.; Wifling, D.; Schnell, D.; Bernhardt, G.; Stark, H.; Seifert, R.; Buschauer, A. Luciferase reporter gene assay on human, murine and rat histamine H_4 receptor orthologs: correlations and discrepancies between distal and proximal readouts. *PLoS One* **2013**, *8*, No. e73961.
(27) Bernat, V.; Heinrich, M. R.; Baumeister, P.; Buschauer, A.; Tschammer, N. Synthesis and application of the first radioligand targeting the allosteric binding pocket of chemokine receptor CXCR3. *ChemMedChem* **2012**, *7*, 1481−1489.
(28) Baumeister, P.; Erdmann, D.; Biselli, S.; Kagermeier, N.; Elz, S.; Bernhardt, G.; Buschauer, A. [^{3}H]UR-DE257: Development of a tritium-labeled squaramide-type selective histamine H_2 receptor antagonist. *ChemMedChem* **2015**, *10*, 83−93.
(29) Cai, H.; Chavez, F.; Dunford, P. J.; Greenspan, A. J.; Meduna, S. P.; Quiroz, J. A.; Savall, B. M.; Tays, K. L.; Thurmond, R. L.; Wei, J.; Wolin, R. L.; Zhang, X. Diamino-pyridine, Pyrimidine, and Pyridazine Modulators of the Histamine H_4 Receptor. WO2009152325A1, 2009; *Chem. Abstr.. 152*, 75050.
(30) Tichenor, M. S. The European Histamine Research Society 43rd Annual Meeting, May 7-10, 2014, Lyon, France. *Inflamm. Res.* **2014**, *63*, 1−48.
(31) Nakao, A.; Suzuki, H.; Ueno, H.; Iwasaki, H.; Setsuta, T.; Kashima, A.; Sunada, S. Discovery and structural analyses of S-adenosyl-L-homocysteine hydrolase inhibitors based on non-adenosine analogs. *Bioorg. Med. Chem.* **2015**, *23*, 4952−4969.
(32) Kraus, A.; Ghorai, P.; Birnkammer, T.; Schnell, D.; Elz, S.; Seifert, R.; Dove, S.; Bernhardt, G.; Buschauer, A. N^G-Acylated aminothiazolylpropylguanidines as potent and selective histamine H_2 receptor agonists. *ChemMedChem* **2009**, *4*, 232−240.
(33) Schreeb, A.; Łażewska, D.; Dove, S.; Buschauer, A.; Kieć-Kononowicz, K.; Stark, H. Histamine H_4 Receptor Ligands. In *Histamine H4 Receptor: A Novel Drug Target in Immunoregulation and Inflammation*; Stark, H., Ed.; Versita: London, 2013; pp 21−62.
(34) Geyer, R.; Kaske, M.; Baumeister, P.; Buschauer, A. Synthesis and functional characterization of imbutamine analogs as histamine H_3 and H_4 receptor ligands. *Arch. Pharm.* **2014**, *347*, 77−88.
(35) Igel, P.; Geyer, R.; Strasser, A.; Dove, S.; Seifert, R.; Buschauer, A. Synthesis and structure-activity relationships of cyanoguanidine-type and structurally related histamine H_4 receptor agonists. *J. Med. Chem.* **2009**, *52*, 6297−6313.
(36) Igel, P.; Schneider, E.; Schnell, D.; Elz, S.; Seifert, R.; Buschauer, A. N^G-Acylated imidazolylpropylguanidines as potent histamine H_4 receptor agonists: selectivity by variation of the N^G-substituent. *J. Med. Chem.* **2009**, *52*, 2623−2627.
(37) Savall, B. M.; Edwards, J. P.; Venable, J. D.; Buzard, D. J.; Thurmond, R.; Hack, M.; McGovern, P. Agonist/antagonist modulation in a series of 2-aryl benzimidazole H_4 receptor ligands. *Bioorg. Med. Chem. Lett.* **2010**, *20*, 3367−3371.
(38) van der Westhuizen, E. T.; Breton, B.; Christopoulos, A.; Bouvier, M. Quantification of ligand bias for clinically relevant β2-adrenergic receptor ligands: implications for drug taxonomy. *Mol. Pharmacol.* **2014**, *85*, 492−509.
(39) Black, J. W.; Leff, P. Operational models of pharmacological agonism. *Proc. R. Soc. London, Ser. B* **1983**, *220*, 141−162.
(40) Black, J. W.; Leff, P.; Shankley, N. P.; Wood, J. An operational model of pharmacological agonism: the effect of E/[A] curve shape on agonist dissociation constant estimation. *Br. J. Pharmacol.* **1985**, *84*, 561−571.
(41) Evans, B. A.; Broxton, N.; Merlin, J.; Sato, M.; Hutchinson, D. S.; Christopoulos, A.; Summers, R. J. Quantification of functional selectivity at the human α_{1A}-adrenoceptor. *Mol. Pharmacol.* **2011**, *79*, 298−307.
(42) Kenakin, T.; Watson, C.; Muniz-Medina, V.; Christopoulos, A.; Novick, S. A simple method for quantifying functional selectivity and agonist bias. *ACS Chem. Neurosci.* **2012**, *3*, 193−203.
(43) Kenakin, T.; Christopoulos, A. Signalling bias in new drug discovery: detection, quantification and therapeutic impact. *Nat. Rev. Drug Discovery* **2013**, *12*, 205−216.
(44) ICRP. Annals of the ICRP. *Recommendations of the International Commission on Radiological Protection. ICRP Publication 26*; Pergamon Press: Oxford, New York, Frankfurt, 1977; Vol. *1* (3).
(45) ICRP. Annals of the ICRP. *The 2007 Recommendations of the International Commission on Radiological Protection. ICRP Publication 103*; Elsevier: 2007; Vol. *37* (2−4).
(46) Pegoli, A.; She, X.; Wifling, D.; Hübner, H.; Bernhardt, G.; Gmeiner, P.; Keller, M. Radiolabeled Dibenzodiazepinone-Type Antagonists Give Evidence of Dualsteric Binding at the M_2 Muscarinic Acetylcholine Receptor. *J. Med. Chem.* **2017**, *60*, 3314−3334.
(47) Pluym, N.; Baumeister, P.; Keller, M.; Bernhardt, G.; Buschauer, A. [^{3}H]UR-PLN196: a selective nonpeptide radioligand and insurmountable antagonist for the neuropeptide Y Y_2 receptor. *ChemMedChem* **2013**, *8*, 587−593.
(48) She, X.; Pegoli, A.; Mayr, J.; Hübner, H.; Bernhardt, G.; Gmeiner, P.; Keller, M. Heterodimerization of dibenzodiazepinone-type muscarinic acetylcholine receptor ligands leads to increased M_2R affinity and selectivity. *ACS Omega* **2017**, *2*, 6741−6754.
(49) Sleight, A. J.; Stam, N. J.; Mutel, V.; Vanderheyden, P. M. L. Radiolabelling of the human 5-HT_{2A} receptor with an agonist, a partial agonist and an antagonist: effects on apparent agonist affinities. *Biochem. Pharmacol.* **1996**, *51*, 71−76.
(50) Brunskole, I.; Strasser, A.; Seifert, R.; Buschauer, A. Role of the second and third extracellular loops of the histamine H_4 receptor in receptor activation. *Naunyn-Schmiedeberg's Arch. Pharmacol.* **2011**, *384*, 301−317.
(51) Yu, F.; Wolin, R. L.; Wei, J.; Desai, P. J.; McGovern, P. M.; Dunford, P. J.; Karlsson, L.; Thurmond, R. L. Pharmacological characterization of oxime agonists of the Histamine H_4 Receptor. *Inflammation Res.* **2010**, *59*, S327.
(52) Aldrich, C.; Bertozzi, C.; Georg, G. I.; Kiessling, L.; Lindsley, C.; Liotta, D.; Merz, K. M., Jr.; Schepartz, A.; Wang, S. The ecstasy and agony of assay interference compounds. *J. Med. Chem.* **2017**, *60*, 2165−2168.
(53) Pop, N.; Igel, P.; Brennauer, A.; Cabrele, C.; Bernhardt, G.; Seifert, R.; Buschauer, A. Functional reconstitution of human neuropeptide Y (NPY) Y_2 and Y_4 receptors in Sf9 insect cells. *J. Recept. Signal Transduction Res.* **2011**, *31*, 271−285.
(54) Hübner, H.; Haubmann, C.; Utz, W.; Gmeiner, P. Conjugated enynes as nonaromatic catechol bioisosteres: synthesis, binding experiments, and computational studies of novel dopamine receptor agonists recognizing preferentially the D_3 subtype. *J. Med. Chem.* **2000**, *43*, 756−762.
(55) Misawa, N.; Kafi, A. K. M.; Hattori, M.; Miura, K.; Masuda, K.; Ozawa, T. Rapid and High-Sensitivity Cell-Based Assays of Protein−Protein Interactions Using Split Click Beetle Luciferase Complementation: An Approach to the Study of G-Protein-Coupled Receptors. *Anal. Chem.* **2010**, *82*, 2552−2560.
(56) Lieb, S.; Littmann, T.; Plank, N.; Felixberger, J.; Tanaka, M.; Schäfer, T.; Krief, S.; Elz, S.; Friedland, K.; Bernhardt, G.; Wegener, J.; Ozawa, T.; Buschauer, A. Label-free versus conventional cellular assays: Functional investigations on the human histamine H_1 receptor. *Pharmacol. Res.* **2016**, *114*, 13−26.
(57) Kagermeier, N.; Werner, K.; Keller, M.; Baumeister, P.; Bernhardt, G.; Seifert, R.; Buschauer, A. Dimeric carbamoylguanidine-type histamine H_2 receptor ligands: a new class of potent and selective agonists. *Bioorg. Med. Chem.* **2015**, *23*, 3957−3969.
(58) Yung-Chi, C.; Prusoff, W. H. Relationship between the inhibition constant (K_i) and the concentration of inhibitor which

DOI: 10.1021/acs.jmedchem.9b01342
J. Med. Chem. XXXX, XXX, XXX−XXX

causes 50 per cent inhibition (I_{50}) of an enzymatic reaction. *Biochem. Pharmacol.* **1973**, *22*, 3099−3108.

DOI: 10.1021/acs.jmedchem.9b01342
J. Med. Chem. XXXX, XXX, XXX−XXX